Elsevier Editorial System(tm) for Energy Conversion and Management
Manuscript Draft

Manuscript Number: ECM-D-18-03229R2

Title: Exergy Analysis and Optimization of a Combined Cooling and Power System Driven by Geothermal Energy for Ice-making and Hydrogen Production

Article Type: Original research paper

Section/Category: 1. Energy Conservation and Efficient Utilization

Keywords: Geothermal, Jaya algorithm, Hydrogen production, ice production

Corresponding Author: Dr. Jiangfeng Wang, Ph.D.

Corresponding Author's Institution: Xi'an Jiaotong University

First Author: Liyan Cao

Order of Authors: Liyan Cao; Juwei Lou; Jiangfeng Wang, Ph.D.; Yiping Dai

Abstract: This paper investigates a combined cooling and power system driven by geothermal energy for ice-making and hydrogen production. The proposed system combines geothermal flash cycle, Kalina cycle, ammonia-water absorption refrigeration cycle and electrolyser. The geothermal energy can be efficiently converted to storable hydrogen and ice. Based on mathematical model, some key parameters are analyzed to figure out their effect on the exergetic performance. An exergy destruction for all components has been performed to find out the distribution of exergy inefficiency. The system exergetic efficiency is optimized by Jaya algorithm and Genetic algorithm and the optimization results are compared. According to the parametric analysis, the exergy efficiency decreases as the back pressure of steam turbine and the back pressure of ammonia-water turbine increase. The exergy efficiency could increase first and then decline, as flash pressure, ammonia-water turbine inlet pressure and ammonia mass fraction of basic solution increase. The optimization results show that the exergy efficiency reaches 23.59%, 25.06% and 26.25% when the geothermal water temperature is 150℃, 160℃ and 170℃. Jaya algorithm has highly precise optimization results.

Dear Editor:

We are sending a manuscript entitled "***Exergy Analysis and Optimization of a Combined Cooling and Power System Driven by Geothermal Energy for Ice-making and Hydrogen Production***", which we should like to submit for publication in ***Energy Conversion and Management***. We investigated a combined cooling and power system driven by geothermal energy for ice-making and hydrogen production. The mathematical model of the system is established to simulate the cycles under steady-state conditions. A parametric analysis of some key parameters is conducted to examine their effects on the system performance. An optimization is conducted by a novel optimization algorithm named Jaya algorithm and Genetic algorithm to obtain the maximum exergy efficiency.

We declare that the manuscript has not been previously published, is not currently submitted for review to any other journal and will not be submitted elsewhere before one decision is made. Its publication is approved by all authors. If accepted, it will not be published elsewhere in the same form, in English or in any other language.

We appreciate your consideration of our manuscript, and we look forward to receiving comments from the reviewers.

Sincerely,

Jiangfeng Wang (on behalf of the authors' team)

Institute of Turbomachinery

Shaanxi Engineering Laboratory of Turbomachinery and Power Equipment

State Key Laboratory of Multiphase Flow in Power Engineering

School of Energy and Power Engineering

Xi’an Jiaotong University, Xi’an, China

Highlights

- A CCP system for ice-making and hydrogen production are proposed.
- The effects of parameters on system performance are examined.
- Optimizations for the CCP system are conducted by Jaya and Genetic algorithm.

Exergy Analysis and Optimization of a Combined Cooling and Power System Driven by Geothermal Energy for Ice-making and Hydrogen Production

Liyan Cao, Juwei Lou, Jiangfeng Wang*, Yiping Dai

Institute of Turbomachinery, Shaanxi Engineering Laboratory of Turbomachinery and Power Equipment, State Key Laboratory of Multiphase Flow in Power Engineering, School of Energy and Power Engineering, Xi'an Jiaotong University, Xi'an 710049, China

Corresponding author: Jiangfeng Wang.

Mailing address:

Institute of Turbomachinery, Shaanxi Engineering Laboratory of Turbomachinery and Power Equipment, State Key Laboratory of Multiphase Flow in Power Engineering, School of Energy and Power Engineering

Xi'an Jiaotong University, Xi'an 710049, China

E-mail address: jfwang@mail.xjtu.edu.cn (JF Wang).

Exergy Analysis and Optimization of a Combined Cooling and Power System Driven by Geothermal Energy for Ice-making and Hydrogen Production

Liyan Cao, Juwei Lou, Jiangfeng Wang*, Yiping Dai

Institute of Turbomachinery, Shaanxi Engineering Laboratory of Turbomachinery and Power Equipment, State Key Laboratory of Multiphase Flow in Power Engineering, School of Energy and Power Engineering, Xi'an Jiaotong University, Xi'an 710049, China

Abstract

This paper investigates a combined cooling and power system driven by geothermal energy for ice-making and hydrogen production. The proposed system combines geothermal flash cycle, Kalina cycle, ammonia-water absorption refrigeration cycle and electrolyser. The geothermal energy can be efficiently converted to storable hydrogen and ice. Based on mathematical model, some key parameters are analyzed to figure out their effect on the exergetic performance. An exergy destruction for all components has been performed to find out the distribution of exergy inefficiency. The system exergetic efficiency is optimized by Jaya algorithm and Genetic algorithm and the optimization results are compared. According to the parametric analysis, the exergy efficiency decreases as the back pressure of steam turbine and the back pressure of ammonia-water turbine increase. The exergy efficiency could increase first and then decline, as flash pressure, ammonia-water turbine inlet pressure and ammonia mass fraction of basic solution increase. The optimization results show that the exergy efficiency reaches 23.59%, 25.06% and 26.25% when the geothermal water temperature is 150℃, 160℃ and 170℃. Jaya algorithm has highly precise optimization results.

Key words: Geothermal, Jaya algorithm, Hydrogen production, ice production

Nomenclature

C	cost rate ($\$\cdot year^{-1}$)
c	costs per unit of exergy ($\$\cdot J^{-1}$);
c_p	specific heat capacity, kJ/(kg K)
E	exergy, kW
HHV	higher heating value, kJ/mol
h	specific enthalpy, kJ/kg
I	exergy destruction, kW
M	molecular weight, g/mol
m	mass flow rate, kg/s
Q	energy, kW
q	quality
s	specific entropy, kJ/(kg K)
T	temperature, K
t	temperature, ℃
V	volumetric flow rate, L/s
VG	vapor generator
W	power, kW
W_y	annual power ($J\cdot year^{-1}$);
x	ammonia mass fraction, %
Z	annually levelized cost value ($\$\cdot year^{-1}$)

Greek letters

ρ	density, kg/m^3
η	efficiency, %
Subscript	
amb	ambient
awt	ammonia-water turbine
basic	ammonia-water basic solution
elec	electrolyser
exg	exergy
F	fuel
gen	generating
geo	geothermal water
H_2	hydrogen
ice	ice
in	inlet
l	liquid
mech	mechanical
motor	motor
net	net
P	product
poor	ammonia-poor solution
poor2	secondary ammonia-poor solution
pump	pump
ref	refrigeration

rich	ammonia-rich vapor
rich2	secondary ammonia-rich vapor
s	isentropic
st	steam turbine
tot	total
v	vapor
1-28	state point

1. Introduction

In recent years, the demand for fossil fuels increases dramatically, which has aroused great concerns about the environmental pollution, greenhouse gas emission and security of energy supply. Different countries have made plans to achieve diversification of energy supply and increase the proportion of renewable energy. Geothermal energy is one of reliable, sustainable and environmentally friendly renewable energy, which has drawn great attention.

Worldwide, geothermal power generation is the most common and efficient method for geothermal utilization. Geothermal power generation technologies in use mainly include flash cycle, binary cycle and flash-binary cycle. Researchers conducted analysis and optimization of the flash cycle [1-3]. The optimization results exhibited the optimum flash pressure to maximize the power output. But the flash cycle requires a relatively high geothermal water temperature. For the geothermal well with low water temperature, Kalina cycle [4-7] is regarded as reliable technologies, since Kalina cycle take full advantage of ammonia-water mixture. Owing to its low-boiling point and temperature slide character, ammonia-water mixture can achieve better thermal match in evaporator to reduce the irreversible loss. On this basis, Kalina cycle has applied as the bottom cycle of flash cycle to raise the thermal and exergy efficiency [8, 9]. The comparison results showed that flash-Kalina cycle generated more power than double-flash cycle did. However, the traditional flash cycle, Kalina cycle or flash-Kalina cycle only generate power, which cannot satisfy the diversified energy demand of users.

The cogeneration systems can supply users with different kinds of energy including electricity, heat and cooling, but more importantly, it has higher energy efficiency. From thermodynamic point of view, cooling is not an easily accessible energy compared to heat. It is usually converted from heat or electricity. Therefore, this brings a focus on the combined power and cooling (CCP) system employing ammonia–water as working fluid. Goswami and Xu [10, 11] came up with a CCP system based on ammonia-water absorption refrigeration cycle. They claimed that this system had potential for efficient recovery of low-grade heat source. Rashidi and Yoo [12] proposed a CCP system that combined the Kalina power cycle and the ejector absorption refrigeration cycle. They compared this new system with another CCP system and found the new system has higher refrigeration output and thermal efficiency. Shokati *et al*. [13] came up with a new CCP system. The proposed cycle was the combination of a Kalina cycle and an absorption refrigeration cycle. Han *et al*. [14] conducted experimental investigation on a combined refrigeration/power generation system. The net power output and cooling output were 1.02kW and 11.67 kW.

However, the energy demand may fluctuate with time. This will trigger the mismatch between energy supply and demand. For lower energy demand, the operation condition of CCP system can be adjusted to meet the change of energy demand, but CCP system will deviate from the design condition and go against the efficient operation. To solve this problem, some researchers try to store electricity energy into hydrogen energy to eliminate the energy mismatch problem. Yüksel [15] conducted thermodynamic analysis for a combined cooling, power and hydrogen production system driven by solar energy. The high temperature water from solar collector drove an Organic rankine cycle and an absorption cooling system to produce electricity and cooling, respectively. A part of electricity was used for hydrogen production by a Proton Exchange Membrane (PEM) electrolyser. Khanmohammadi *et al*. [16] proposed a similar combined cooling, power and hydrogen production system and carried out a parametric study to determine the main design parameters and their effects on the system performance. Akrami *et al*. [17] proposed multi-generation system comprised of a geothermal based organic Rankine cycle, domestic water heater, absorption refrigeration cycle and PEM electrolyser. The geothermal water was used to drive ORC and to heat the domestic water up, successively. A part of power generated by organic turbine was used for hydrogen production and organic turbine exhaust was used as the heat source of absorption refrigeration cycle. Yuksel *et al.* [18] came up with a novel integrated geothermal energy-based system for cooling and hydrogen production. The cooling and hydrogen was produced by an absorption refrigeration cycle and PEM electrolyser, separately. They claimed that the energetic and exergetic efficiencies of the integrated system could reach to 42.59% and 48.24%, respectively. Parham *et al*. [19] proposed a novel multi-generation system including an open absorption heat transformer, an ORC and an electrolyser for hydrogen production. They analyzed the system from both first and second laws of thermodynamics. Boyaghchi and Safari [20] proposed a new designed quadruple energy production system integrated with geothermal energy, which could produce electricity power, heating, cooling and hydrogen. They conducted thermoeconomic analysis and optimization for the system, and found that the total avoidable investment cost rate is improved within 17.4% relative to the base point. Ahmadi *et al*. [21] proposed a multigeneration energy system to produce power, heating, cooling, hot water and hydrogen. They performed multi-objective optimization for the system and determined the optimum thermoeconomic performance.

All the combined cooling, power and hydrogen systems could convert electricity to hydrogen that can be easily stored to counter the mismatch between supply and demand. However, these papers don't take the cooling mismatch into consideration. In addition, all the systems generate electricity and cooling with separate cycles, and different cycles run with different working medium. As a result, the systems have very complex configurations. We believe that the cogeneration system could have a more compact configuration and all the products are storable. Toward this end, we propose a combined cooling and power system driven by geothermal energy for ice-making and hydrogen production in this paper. The system consists of a top geothermal flash cycle, a bottom combined cooling and power cycle as well as an electrolyser. For the bottom cycle, both Kalina cycle and absorption refrigeration cycle can adopt ammonia-water as working fluid, we integrate Kalina cycle with absorption refrigeration cycle by sharing same key components to simplify the system configuration. And electricity and cooling are converted to storable hydrogen and ice, respectively. We also conduct a parametric analysis to study the effect of key parameters on system performance. In addition, we use a novel optimization algorithm named Jaya algorithm to optimize the systems and compare the Jaya algorithm with Genetic algorithm to verify its accuracy.

2. System description

Fig. 1 shows the schematic diagram of a combined cooling and power system for ice-making and hydrogen production. The high-temperature geothermal water is pumped from geothermal well to flashing devise in which the geothermal water is decompressed and partially becomes steam. The steam expands in steam turbine and the exhaust leaves turbine with low temperature and low pressure. The remaining water from flashing devise is used to vaporize the ammonia-water basic solution in vapor generator (VG), and then the water is mixed with steam turbine exhaust and delivered to recharge well. The vaporized ammonia-water basic solution is delivered to separator 1, in which it is separated into ammonia-rich vapor and ammonia-poor solution. After expanding in ammonia-water turbine to generate electrical power, the ammonia-water turbine exhaust is separated into secondary ammonia-rich vapor and secondary ammonia-poor solution in separator 2. The secondary ammonia-rich vapor is condensed and throttled down to generate cold energy in evaporator. The generated cold energy is used to produce ice. The secondary ammonia-poor solution from separator 2, the secondary ammonia-rich vapor from evaporator and the ammonia-poor solution from separator 1 are mixed and condensed into supercooling ammonia-water basic solution in condenser 2. The ammonia-water basic solution is preheated in regenerator 1 and regenerator 2. Finally, the ammonia-water basic solution is delivered to VG to complete the bottom cycle. All the power generated by turbines is given to electrolyser to break the molecules of water into hydrogen and oxygen.

3. Mathematical model and performance criteria

The mathematical model is established based on mass and energy conservation. To simplify the mathematical model, some assumptions are applied as follows:

(1) The system is simulated in steady state.

(2) The flows across the throttle valve are isenthalpic.

(3) The working fluid is condensed to saturated liquid in condenser.

(4) The pressure loss and heat loss are neglected.

(5) Turbines and pumps have isentropic efficiency.

3.1 Mathematical model

For the flashing devise, the mass and energy balance equations are described as:

$$\frac{m_{\mathrm{v}}}{m_{\mathrm{geo}}} = \frac{h_1 - h_3}{h_2 - h_3} \tag{1}$$

$$m_{\mathrm{geo}} = m_l + m_{\mathrm{v}} \tag{2}$$

For the VG, energy balance equation is expressed as:

$$m_{\mathrm{l}}(h_3 - h_4) = m_{\mathrm{basic}}(h_7 - h_9) \tag{3}$$

For the steam turbine, the isentropic expansion efficiency is represented as:

$$s_2 = s_{5\mathrm{s}} \tag{4}$$

$$\eta_{\mathrm{st}} = \frac{h_2 - h_5}{h_2 - h_{5\mathrm{s}}} \tag{5}$$

For the separator 1, the mass and energy balance equation are written as:

$$m_{\mathrm{basic}} = m_{\mathrm{rich}} + m_{\mathrm{poor}} \tag{6}$$

$$m_{\mathrm{basic}} x_7 = m_{\mathrm{rich}} x_8 + m_{\mathrm{poor}} x_9 \tag{7}$$

$$m_{\mathrm{basic}} h_7 = m_{\mathrm{rich}} h_8 + m_{\mathrm{poor}} h_9 \tag{8}$$

For the ammonia-water turbine, isentropic expansion efficiency can be expressed as:

$$s_8 = s_{10s} \tag{9}$$

$$\eta_{awt} = \frac{h_8 - h_{10}}{h_8 - h_{10s}} \tag{10}$$

For the evaporator, the energy balance equation is given by:

$$m_{rich2}(h_{17} - h_{16}) = m_{water}(h_{23} - h_{24}) \tag{11}$$

For the heat regenerator 1, the energy balance equation is defined as:

$$m_{basic}(h_{20} - h_{19}) = m_v(h_5 - h_6) \tag{12}$$

For the heat regenerator 2, the energy balance equation is described as follows:

$$m_{basic}(h_{25} - h_{20}) = m_{poor2}(h_9 - h_{13}) \tag{13}$$

For the evaporator, the mass and energy balance equations are as follows:

$$m_{rich} = m_{rich2} + m_{poor2} \tag{14}$$

$$m_{rich}h_{10} = m_{rich2}h_{11} + m_{poor2}h_{12} \tag{15}$$

The isenthalpic flow across the throttle valves has the form:

$$h_{13} = h_{14} \tag{16}$$

$$h_{15} = h_{16} \tag{17}$$

$$h_{12} = h_{26} \tag{18}$$

The power consumption and isentropic efficiency of pumps are defined as:

$$\eta_{pump} = \frac{h_{19s} - h_{18}}{h_{19} - h_{18}} \tag{19}$$

$$\eta_{pump} = \frac{h_{22s} - h_{21}}{h_{22} - h_{21}} \tag{20}$$

$$W_{pump} = (h_{19} - h_{18})m_{basic} + (h_{22} - h_{21})m_v \tag{21}$$

The electric power generated by turbine is given by:

$$W_{\mathrm{st}} = m_{\mathrm{v}}(h_2 - h_5) \tag{22}$$

$$W_{\mathrm{awt}} = \left[m_{\mathrm{rich}}(h_8 - h_{10})\right] \tag{23}$$

$$W_{\mathrm{net}} = \left(W_{\mathrm{st}} + W_{\mathrm{awt}}\right)\eta_{\mathrm{mech}}\eta_{\mathrm{gen}} - W_{\mathrm{pump}} / \eta_{\mathrm{pump,motor}} \tag{24}$$

where η_{mech}, η_{gen} and $\eta_{\mathrm{pump,motor}}$ are mechanical efficiency, generator efficiency and pump motor efficiency, respectively.

In this paper, all the power is used to produce hydrogen by electrolysis. The Higher Heating Value (*HHV*) of hydrogen is 285.840 kJ/mol. That's to say, burning one mold of hydrogen would produce one mole of water and release 285.840kJ of heat. Ideally, electrolyzing one mole of water to produce one mole of hydrogen will consumes 285.840kJ of heat [22].

$$4\mathrm{H_2O} + 4\mathrm{e}^- = 2\mathrm{H_2}\uparrow + 4\mathrm{OH}^- \tag{25}$$

$$4\mathrm{OH}^- - 4\mathrm{e}^- = 2\mathrm{H_2O} + \mathrm{O_2}\uparrow \tag{26}$$

In this paper, an alkaline electrolyser is chosen to produce hydrogen. The total efficiency of the electrolyser is 77%, which has taken energy dissipations of AC/DC converter and other equipment into consideration [22]. The hydrogen production is given by

$$V_{\mathrm{H_2}} = \frac{W_{\mathrm{net}} \cdot 1000 \cdot M_{\mathrm{H_2}} \cdot \eta_{\mathrm{elec}}}{HHV \cdot \mathrm{V}_{\mathrm{H_2}} \cdot \rho_{\mathrm{H_2}}} \tag{27}$$

where $V_{\mathrm{H_2}}$, $M_{\mathrm{H_2}}$, $\rho_{\mathrm{H_2}}$ and η_{elec} are volumetric flow rate of hydrogen, molecular weight of hydrogen, density of hydrogen and efficiency of the electrolyser, respectively.

The cold energy generated by evaporator to make ice is defined as:

$$Q_{\text{ref}} = m_{\text{ice}} c_{\text{p}} (T_{23} - T_{24}) \tag{28}$$

where m_{ice} is the ice production rate.

3.2 Performance criteria

The thermodynamic performance of system is evaluated by system exergy efficiency and hydrogen exergy efficiency. The exergy is given by:

$$E = (h - h_{\text{amb}}) - T_{\text{amb}} (s - s_{\text{amb}}) \tag{29}$$

The cold exergy is written as:

$$E_{\text{ref}} = T_{\text{amb}} (s - s_{\text{amb}}) - (h - h_{\text{amb}}) \tag{30}$$

The exergy of hydrogen approximately equals to the HHV of H_2, namely 285.840 kJ/mol [22].

The system exergy efficiency is expressed as:

$$\eta_{\text{exg}} = \frac{E_{\text{H}_2} + E_{\text{ref}}}{E_{\text{in}}} \tag{31}$$

The hydrogen efficiency is expressed as:

$$\eta_{\text{exg-H}_2} = \frac{E_{\text{H}_2}}{E_{\text{in}}} \tag{32}$$

E_{in} is the exergy input defined as:

$$E_{\text{in}} = m_{\text{geo}} E_1 - m_l E_4 - m_{\text{v}} E_{22} \tag{33}$$

The exergy destruction is defined as follows.

$$I = \Delta_{\text{out}}^{\text{in}} E \tag{34}$$

3.3. Mathematical model validation

Essentially, our proposed system is a combination of three cycles: a geothermal flash cycle, a Kalina cycle with a backpressure turbine and an absorption refrigeration cycle. To verify the feasibility of this combination, we conducted a mathematical model validation. Three parts of the proposed system are respectively validated with data in open literature [23-25]. Tables 1 to 3 demonstrate the validation results, and the simulation results are well consistent with the data in literature.

4. Results and discussion

In this section, a parametric analysis for the combined cooling and power system for ice-making and hydrogen production is performed. Some key parameters (e.g. flash pressure, ammonia mass fraction of basic solution, ammonia-water turbine inlet pressure, ammonia-water turbine back pressure, steam turbine back pressure) are analyzed to figure out their effect on the system performance. Note that the pinch point temperature difference is a constant. The thermodynamic properties of working fluid are calculated by REFPROP 9.1 developed by the National Institute of Standard and Technology (NIST) of the United States. The simulation of the system is conducted by MATLAB software. To ensure the operation safety, quality of turbine exhaust should not be lower than 0.88 [26]. All the analyses are subject to this restriction. To satisfy the requirement of ice-making, the evaporating temperature and ice temperature are -13℃[27] and -5℃[28], respectively.

The simulation boundary condition and simulation results are listed in Table 4 and Table 5. Table 6 demonstrates the thermodynamic parameters of each node under simulation condition. Fig. 2 illustrates the exergy destruction distribution of critical components under simulation condition.

Fig. 2 shows the exergy destruction of different components. The largest exergy destruction takes place in condensers, which is mainly caused by large heat transfer temperature differences. The exergy destruction of steam turbine and ammonia-water turbine are 15.99%. Heat regenerators contribute 14.72% of total exergy destruction. For VG & evaporator, valves, separators and other components, the exergy destruction is 7.89%, 7.04%, 5.56% and 7.11%, respectively.

4.1. Parametric analysis

Fig. 3 shows the effect of flash pressure on system performance. As the flash pressure increases, the mass flow rate of steam decreases, leading to a decrease in the power output of steam turbine. Meanwhile, the mass flow rate of water from flashing device increases with flash pressure. As a result, it will provide more heat to bottom cycle and lead to an increase in mass flow rate of ammonia-water basic solution. The mass flow rate of ammonia-rich vapor and the power output of ammonia-water turbine increase as well. Under the comprehensive impact of steam turbine and ammonia-water turbine, the net power output of the system firstly increases and then decreases. Thus, the hydrogen production has the same variation with net power output when the flash pressure increases. The increment of the mass flow rate of secondary ammonia-rich vapor results in the increase in refrigeration exergy. Therefore, the ice production increases. Note that the hydrogen production increases firstly and then decreases, the variation of hydrogen exergy efficiency also shows a convex curve. According to Eq. (31), system exergy efficiency is determined by hydrogen exergy, refrigeration exergy and total exergy input. Note that the refrigeration exergy is negligibly small and has little impact on exergy efficiency comparing with hydrogen exergy. As a result, the variation of system exergy efficiency is also a convex curve. Note that q_5 and q_{10} refer to the qualities of steam turbine exhaust and ammonia-water turbine exhaust. The qualities are both higher than 0.88. It won’t cause severe erosion of turbine blades.

Fig. 4 shows the effect of steam turbine back pressure on the system performance. Note that the bottom cycle is independent of the steam turbine back pressure, the mass flow rate of ammonia-water basic solution, the power output of ammonia-water turbine, the refrigeration exergy and ice production won't change with variation of the steam turbine back pressure. Meanwhile, the increment of steam turbine back pressure causes a decrease in power output of steam turbine. Consequently, the decreasing net power output of the system results in the decreasing hydrogen production of the system. The hydrogen exergy efficiency and system exergy efficiency decrease as well. The qualities of steam turbine exhaust and ammonia-water turbine exhaust are higher than 0.88 when steam turbine back pressure varies.

Fig. 5 shows the effect of ammonia mass fraction of basic solution on system performance. When the ammonia mass fraction of basic solution increases, the power output of steam turbine remains unchanged and the mass flow rate of ammonia-rich vapor and secondary ammonia-rich vapor rise simultaneously, which enables the net power output, the hydrogen production, the refrigeration exergy and ice production increase, simultaneously. Meanwhile, the energy and exergy input increase with ammonia mass fraction of basic solution significantly. According to Eq. (31) and (32), the hydrogen exergy efficiency and system exergy efficiency both show the convex curves under the combined impact of increasing exergy input, hydrogen production and refrigeration exergy. The qualities of steam turbine exhaust and ammonia-water turbine exhaust lie in safety zone.

Fig. 6 shows the effect of ammonia-water turbine inlet pressure on system performance. The flash cycle is independent of ammonia-water turbine inlet pressure.

Thus, the power output of steam turbine remains unchanged. When the ammonia-water turbine inlet pressure increases, the variation of the specific enthalpy drop in ammonia-water turbine is opposite to that of the mass flow rate of ammonia-rich vapor. Under the impact of these two factors, the net power output of the system as well as the hydrogen production firstly increases and then decreases. In addition, the mass flow rate of secondary ammonia-rich vapor decrease, which causes a decrease in refrigeration exergy and ice production. Comparing with hydrogen exergy, the impact of refrigeration exergy on system exergy efficiency is negligibly small. Dominated by hydrogen exergy, both hydrogen exergy efficiency and system exergy efficiency increase first and then decrease. The qualities of steam turbine exhaust and ammonia-water turbine exhaust won’t cause severe erosion of turbine blades.

Fig. 7 shows the effect of ammonia-water turbine back pressure on system performance. As the ammonia-water turbine back pressure increases, the mass flow rates of basic solution and ammonia-rich vapor remain unchanged, and the enthalpy drop through ammonia-water turbine decreases. This causes a decrease in power output of ammonia-water turbine. Meanwhile, the power output of steam turbine keeps unchanged. Therefore, the net power output of the system decreases, which leads to the decline of hydrogen production. The refrigeration exergy and ice production decrease since the mass flow rate of secondary ammonia-rich solution decreases. Influenced by the decrease in hydrogen exergy and refrigeration exergy, the hydrogen exergy efficiency and system exergy efficiency decline. The qualities of steam turbine exhaust and ammonia-water turbine exhaust are acceptable.

4.2. Optimization

According to the parametric analysis, there may be an optimum performance for the combined cooling and power system driven by geothermal energy for ice-making and hydrogen production. Thus, a performance optimization is conducted to obtain the maximum system exergy efficiency. There are many optimization methods, such as Genetic algorithm (GA), Teaching-learning-based optimization (TLBO), Evolution Strategy (GE) and Evolution Programming (EP). For the performance optimization of the system driven by low temperature heat source, GA is the most commonly used optimization method for its global optimization ability [29-31].

Recently, Rao and Waghmare [32] proposed a new optimization algorithm named Jaya algorithm (JA). Unlike other algorithms, JA requires only the common control parameters such as population size, number of generations and elite size to run the optimization algorithm. And other algorithms require common control parameters as well as their own algorithm-specific parameters, which could add complexity to the algorithms [32]. The author tested JA and other several optimization algorithms on 21 benchmark problems related to constrained design optimization and claimed that JA could get highly precise optimization results with less computational time. The brief introduction of JA is as follows.

The objective function $f(x)$, which is a function of m design variables (j=1,2,…,m), is to be maximized and minimized by JA. At any i^{th} generation, there are n candidate solutions associated with n populations (k=1,2,…,n). And $x_{j,k,i}$ is the j^{th} variable in k^{th} population at i^{th} generation. The best value and worst value among n candidate solutions at i^{th} generation are $f(x)_{best,i}$ and $f(x)_{worst,i}$. Therefore, $x_{j,best,i}$ is the j^{th} variable in the population that corresponds to the best candidate solution $f(x)_{best,i}$, and $x_{j,worst,i}$ is the j^{th} variable in the population that corresponds to the worst candidate solution $f(x)_{worst,i}$ at i^{th} generation. For $(i+1)^{th}$ generation, x is modified as,

$$x_{j,k,i+1} = x_{j,k,i} + r_{1,j,i}(x_{j,best,i} - |x_{j,k,i}|) - r_{2,j,i}(x_{j,worst,i} - |x_{j,k,i}|) \qquad (35)$$

where $r_{1,j,i}$ and $r_{2,j,i}$ both are the random numbers between 0 and 1. The Flow chart of Jaya algorithm is showed in Fig. 8.

To verify the optimization accuracy of JA algorithm, a system performance optimization is conducted by using both JA and GA with the same boundary condition and common control parameters. It is noted that the system is optimized under three different geothermal water temperatures (150 ℃, 160 ℃ and 170 ℃) to guarantee reliability of results. For each geothermal water temperature, the optimizations with JA and GA are performed with three and five different population size, respectively. The optimization with JA is carried out using the program written in Matlab by authors. The optimization with GA is performed by Matlab optimization tool box. All optimizations are running in the completely same computing environment. The operation parameters of optimization algorithm and ranges of key thermodynamic parameters are listed in Table 7 and the optimization results are listed in Table 8.

For each geothermal water temperature, the optimum exergy efficiencies calculated by JA are the same under three different population sizes. The exergy efficiencies are 23.59%, 25.06% and 26.25% when geothermal water temperatures are 150℃, 160℃ and 170℃. These results are almost equal to those calculated by GA with population sizes of 50 and 100. Note that small population size leads to inaccurate results of GA. That’s to say, JA gets accurate results with less population and has potential to save computational time.

To verify the thermoeconomic feasibility, we have conducted thermoeconomic estimation for the proposed system under optimum performance conditions. In this paper, all exchangers are plate heat exchangers (PHE) and separators are vertical cyclone type. The heat transfer correlations and size estimation model for PHEs and separators are demonstrated in Ref. [33]. The *module costing technique* [34] is used to estimate the equipment costs, and the *exergy costing approach* [34] is applied to calculate the cost of product. We assume the lifespan (n) and annual working hours (t_{y}) of the proposed system are 25 years and 4000 hours, respectively. The annual cost balance is given by

$$C_{\mathrm{P,tot}} = C_{\mathrm{F,tot}} + Z_{\mathrm{tot}}$$

where $C_{\mathrm{P,tot}}$ is annual product cost rate, $C_{\mathrm{F,tot}}$ is annual fuel cost rate, Z_{tot} is the annually levelized cost of equipment. The annual product cost per unit of exergy output is expressed as

$$c_{\mathrm{P,tot}} = \frac{C_{\mathrm{P,tot}}}{E_{\mathrm{P,tot}}} = \frac{C_{\mathrm{P,tot}}}{W_{\mathrm{y,net}} + E_{\mathrm{y,ref}}}$$

where the $W_{\mathrm{y,net}}$ is the annual net power output and $E_{\mathrm{y,ref}}$ is the annual cold exergy output.

$$E_{\mathrm{y,ref}} = E_{\mathrm{ref}} \cdot 3600 \cdot t_{\mathrm{y}}$$

$$W_{\mathrm{y,net}} = W_{\mathrm{net}} \cdot 3600 \cdot t_{\mathrm{y}}$$

The specific thermoeconomic models are demonstrated in Ref. [35]. Table 9 shows the results of thermoeconomic estimation under optimum performance condition.

As the temperature of geothermal water increases, the annual product cost rate increases and the annual product cost per unit of exergy output decreases.

5. Conclusions

In this paper, we propose a combined ice-making and hydrogen production system. We investigate the exergy destruction of different components and analyze the effect of key parameters on system performance. We also conduct an optimization with JA and GA to search for maximum exergy efficiencies under three different geothermal water temperatures. The main conclusions are as follow:

(1) The condensers contribute most to the exergy destruction owing to the high temperature difference. The exergy efficiency decreases as back pressure of steam turbine and ammonia-water turbine increase. And exergy efficiency shows a convex curve, as flash pressure, ammonia-water turbine inlet pressure and ammonia mass fraction of basic solution increase.

(2) The optimum exergy efficiencies calculated by JA are about 23.59%, 25.06% and 26.25% for geothermal water temperature of 150℃, 160℃ and 170℃, respectively. JA could get highly precise optimization results with less population size.

Acknowledgements

The authors gratefully acknowledge the financial support by the National Natural Science Foundation of China (Grant No. 51476121).

References

[1] S. Amiri, H. Shokouhmand, A. Kahrobaian, S. Amiri. Optimum flashing pressure in single and double flash geothermal power plants. ASME 2008 Heat Transfer Summer Conference collocated with the Fluids Engineering, Energy Sustainability,

and 3rd Energy Nanotechnology Conferences. American Society of Mechanical Engineers2008. pp. 125-9.

[2] Y. Cerci. Performance evaluation of a single-flash geothermal power plant in Denizli, Turkey. Energy. 28 (2003) 27-35.

[3] N.A. Pambudi, R. Itoi, S. Jalilinasrabady, K. Jaelani. Exergy analysis and optimization of Dieng single-flash geothermal power plant. Energ Convers Manage. 78 (2014) 405-11.

[4] M. Fallah, S.M.S. Mahmoudi, M. Yari, R.A. Ghiasi. Advanced exergy analysis of the Kalina cycle applied for low temperature enhanced geothermal system. Energ Convers Manage. 108 (2016) 190-201.

[5] D. Fiaschi, G. Manfrida, E. Rogai, L. Talluri. Exergoeconomic analysis and comparison between ORC and Kalina cycles to exploit low and medium-high temperature heat from two different geothermal sites. Energ Convers Manage. 154 (2017) 503-16.

[6] E. Wang, Z. Yu, F. Zhang. Investigation on efficiency improvement of a Kalina cycle by sliding condensation pressure method. Energ Convers Manage. 151 (2017) 123-35.

[7] H. Saffari, S. Sadeghi, M. Khoshzat, P. Mehregan. Thermodynamic analysis and optimization of a geothermal Kalina cycle system using Artificial Bee Colony algorithm. Renew Energ. 89 (2016) 154-67.

[8] L. Cao, J. Wang, P. Zhao, Y. Dai. Thermodynamic comparison among double-flash flash-Kalina and flash-ORC geothermal power plants. International Journal of Thermodynamics. 19 (2016) 53-60.

[9] J. Wang, J. Wang, Y. Dai, P. Zhao. Thermodynamic analysis and optimization of a flash-binary geothermal power generation system. Geothermics. 55 (2015) 69-77.

[10] D.Y. Goswami, F. Xu. Analysis of a new thermodynamic cycle for combined power and cooling using low and mid temperature solar collectors. Journal of Solar Energy Engineering. 121 (1999) 91-7.

[11] F. Xu, D.Y. Goswami, S.S. Bhagwat. A combined power/cooling cycle. Energy. 25 (2000) 233-46.

[12] J. Rashidi, C. Yoo. A novel Kalina power-cooling cycle with an ejector absorption refrigeration cycle: Thermodynamic modelling and pinch analysis. Energ Convers Manage. 162 (2018) 225-38.

[13] N. Shokati, F. Ranjbar, M. Yari. A comprehensive exergoeconomic analysis of absorption power and cooling cogeneration cycles based on Kalina, part 1: Simulation. Energ Convers Manage. 158 (2018) 437-59.

[14] W. Han, Q. Chen, L. Sun, S. Ma, T. Zhao, D. Zheng, et al. Experimental studies on a combined refrigeration/power generation system activated by low-grade heat. Energy. 74 (2014) 59-66.

[15] Y.E. Yüksel. Thermodynamic assessment of modified Organic Rankine Cycle integrated with parabolic trough collector for hydrogen production. International Journal of Hydrogen Energy. (2017).

[16] S. Khanmohammadi, P. Heidarnejad, N. Javani, H. Ganjehsarabi. Exergoeconomic analysis and multi objective optimization of a solar based integrated energy system for hydrogen production. international journal of hydrogen energy. 42 (2017) 21443-53.

[17] E. Akrami, I. Khazaee, A. Gholami. Comprehensive analysis of a multi-generation energy system by using an energy-exergy methodology for hot water, cooling, power and hydrogen production. Applied Thermal Engineering. 129 (2018) 995-1001.

[18] Y.E. Yuksel, M. Ozturk, I. Dincer. Thermodynamic analysis and assessment of a novel integrated geothermal energy-based system for hydrogen production and storage. International Journal of Hydrogen Energy. (2017).

[19] K. Parham, H. Alimoradiyan, M. Assadi. Energy, exergy and environmental analysis of a novel combined system producing power, water and hydrogen. Energy. 134 (2017) 882-92.

[20] F.A. Boyaghchi, H. Safari. Parametric study and multi-criteria optimization of total exergetic and cost rates improvement potentials of a new geothermal based quadruple energy system. Energ Convers Manage. 137 (2017) 130-41.

[21] P. Ahmadi, I. Dincer, M.A. Rosen. Thermodynamic modeling and multi-objective evolutionary-based optimization of a new multigeneration energy system. Energ Convers Manage. 76 (2013) 282-300.

[22] Z.X. Sun, J.F. Wang, Y.P. Dai, J.H. Wang. Exergy analysis and optimization of a hydrogen production process by a solar-liquefied natural gas hybrid driven transcritical CO2 power cycle. International Journal of Hydrogen Energy. 37 (2012) 18731-9.

[23] A. Mohammadi, M. Mehrpooya. Energy and exergy analyses of a combined desalination and CCHP system driven by geothermal energy. Applied Thermal Engineering. 116 (2017) 685-94.

[24] A.D. Pasek, T.F. Soelaiman, C. Gunawan. Thermodynamics study of flash–binary cycle in geothermal power plant. Renewable and sustainable energy reviews. 15 (2011) 5218-23.

[25] H. Rostamzadeh, H. Ghaebi, T. Parikhani. Thermodynamic and thermoeconomic analysis of a novel combined cooling and power (CCP) cycle. Applied Thermal Engineering. 139 (2018) 474-87.

[26] A. Ganjehkaviri, M.M. Jaafar, S. Hosseini. Optimization and the effect of steam turbine outlet quality on the output power of a combined cycle power plant. Energ Convers Manage. 89 (2015) 231-43.

[27] http://www.omt-icemachines.com/temperature-factors-of-ice-machine.html.

[28] http://www.omt-icemachines.com/25t-flake-ice-machine.html.

[29] H.M. Hettiarachchi, M. Golubovic, W.M. Worek, Y. Ikegami. Optimum design criteria for an organic Rankine cycle using low-temperature geothermal heat sources. Energy. 32 (2007) 1698-706.

[30] S. Quoilin, M. Van Den Broek, S. Declaye, P. Dewallef, V. Lemort. Techno-economic survey of Organic Rankine Cycle (ORC) systems. Renewable and Sustainable Energy Reviews. 22 (2013) 168-86.

[31] D. Wei, X. Lu, Z. Lu, J. Gu. Performance analysis and optimization of organic Rankine cycle (ORC) for waste heat recovery. Energ Convers Manage. 48 (2007) 1113-9.

[32] R.V. Rao, G. Waghmare. A new optimization algorithm for solving complex constrained design optimization problems. Engineering Optimization. 49 (2017) 60-83.

[33] L. Cao, J. Wang, L. Chen, Y. Dai. Comprehensive analysis and optimization of Kalina-Flash cycles for low-grade heat source. Applied Thermal Engineering. 131 (2018) 540-52.

[34] R. Turton. Analysis, synthesis, and design of chemical processes. 4th ed. Prentice Hall, Upper Saddle River, NJ, 2012.

[35] Y. Zhao, J. Wang, L. Cao, Y. Wang. Comprehensive analysis and parametric optimization of a CCP (combined cooling and power) system driven by geothermal source. Energy. 97 (2016) 470-87.

Figure captions

Fig. 1 The schematic diagram of a combined cooling and hydrogen production system

Fig. 2 Exergy destruction of different components

Fig. 3 The effect of flash pressure on system performance

Fig. 4 The effect of steam turbine back pressure on the system performance

Fig. 5 The effect of ammonia mass fraction of basic solution on system performance

Fig. 6 The effect of ammonia-water turbine inlet pressure on system performance

Fig. 7 The effect of ammonia-water turbine back pressure on system performance

Fig. 8 The Flow chart of Jaya algorithm

Table 1 Mathematical model validation for flash cycle; (a) Present work, (b) Ref. [24].

State	*t* (℃)		*P* (kPa)		*m* (kg/s)	
	(a)	(b)	(a)	(b)	(a)	(b)
1	170.00	170.00	901.30	901.30	111.10	111.10
2	158.82	158.90	600.00	600.00	2.60	2.73
3	158.82	158.90	600.00	600.00	108.50	108.37
5	76.52	76.69	41.30	41.30	2.60	2.73

Table 2 Mathematical model validation for Kalina cycle with backpressure turbine; (a) Present work, (b) Ref. [25].

State	*t* (℃)		*P* (kPa)		*m* (kg/s)		*x* (%)	
	(a)	(b)	(a)	(b)	(a)	(b)	(a)	(b)
7	199.95	199.95	2000.00	2000.00	0.77	0.77	15.00	15.00
8	199.95	199.95	2000.00	2000.00	0.45	0.43	22.23	23.20
9	199.95	199.95	2000.00	2000.00	0.32	0.34	4.48	4.70
10	177.86	177.85	1235.00	1235.00	0.45	0.43	22.23	23.20

Table 3 Mathematical model validation for absorption refrigeration cycle; (a) Present work, (b) Ref. [23].

State	*t* (℃)		*P* (kPa)		*m* (kg/s)		*x* (%)	
	(a)	(b)	(a)	(b)	(a)	(b)	(a)	(b)
10	126.91	126.91	700.00	700.00	0.1440	0.1440	67.00	67.00
11	126.91	126.91	700.00	700.00	0.1429	0.1420	67.41	68.00
12	126.91	126.91	700.00	700.00	0.0011	0.0020	13.24	14.00
15	29.03	28.61	700.00	700.00	0.1429	0.1420	67.41	68.00
16	-3.02	-3.28	200.00	200.00	0.1429	0.1420	67.41	68.00
17	10.00	10.00	200.00	200.00	0.1429	0.1420	67.41	68.00
26	92.54	92.18	200.00	200.00	0.0011	0.0020	13.24	14.00

Table 4 Simulation conditions of system

Term	Value
Environment pressure (kPa)	101.33
Environment temperature (℃)	20.00
Geothermal water temperature (℃)	170.00
Geothermal water mass flow ($kg\cdot s^{-1}$)	30.00
Pinch point temperature difference (℃)	10.00
Approach point temperature difference (℃)	7.00
Evaporating temperature (℃) [27]	-13.00
Ice temperature (℃) [28]	-5.00
Turbine isentropic efficiency (%)	75.00
Pump isentropic efficiency (%)	65.00
Mechanical efficiency (%)	96.00
Generating efficiency (%)	95.00
Pump motor efficiency (%)	95.00
Alkaline electrolyser total efficiency (%)	77.00
Flash pressure (kPa)	450.00
Steam turbine back pressure (kPa)	30.00
Ammonia mass fraction of basic solution (%)	40.00
Ammonia-water turbine inlet pressure (kPa)	2500.00
Ammonia-water turbine back pressure (kPa)	1200.00

Table 5 System performance

Term	Value
Power of steam turbine (kW)	363.56
Power of ammonia-water turbine (kW)	110.83
Quality of steam turbine exhaust	0.92
Quality of ammonia-water turbine exhaust	0.97
Power consumption of pumps (kW)	60.28
Net power output (kW)	414.10
Hydrogen production (L/s)	24.82
Refrigeration capacity (kW)	837.66
Refrigeration exergy (kW)	34.25
Ice-making capacity (kg/s)	7.25
Hydrogen production exergy efficiency (%)	18.28
System exergy efficiency (%)	20.24

Table 6 Thermodynamic parameters of each node under simulation condition

State	t (℃)	P (kPa)	x (%)	h (kJ·kg^{-1})	m (kg·s^{-1})	quality
1	170.00	1000.00	0.00	719.20	30.00	0.00
2	147.90	450.00	0.00	2743.39	1.36	1.00
3	147.90	450.00	0.00	623.14	28.64	0.00
4	127.38	450.00	0.00	535.35	28.64	0.00
5	69.10	30.00	0.00	2420.31	1.36	0.91
6	69.10	30.00	0.00	1480.17	1.36	0.51
7	139.90	2500.00	40.00	728.54	9.46	0.13
8	139.90	2500.00	88.60	1964.55	1.27	1.00
9	139.90	2500.00	32.44	536.34	8.19	0.00
10	111.38	1200.00	88.60	1869.07	1.27	0.97
11	111.38	1200.00	90.60	1918.81	1.23	1.00
12	111.38	1200.00	29.27	395.09	0.04	0.00
13	69.10	2500.00	32.44	200.70	8.19	0.00
14	51.41	228.32	32.44	200.70	8.19	0.05
15	34.40	1200.00	90.60	400.15	1.23	0.00
16	-13.00	228.32	90.60	400.15	1.23	0.17
17	-6.00	228.32	90.60	1080.57	1.23	0.67
18	31.08	228.32	40.00	32.97	9.46	0.00
19	31.57	2500.00	40.00	37.06	9.46	0.00
20	61.10	2500.00	40.00	172.18	9.46	0.00

21	69.10	30.00	0.00	289.27	1.36	0.00
22	69.17	450.00	0.00	289.93	1.36	0.00
23	12.00	101.32	0.00	50.51	7.25	0.00
24	-5.00	101.32	0.00	21.12	7.25	0.00
25	121.76	2500.00	40.00	462.65	9.46	0.00
26	67.99	228.32	29.27	395.09	0.04	0.12
27	47.01	228.32	40.00	316.10	9.46	0.13

Table 7 Operation parameters of optimization algorithm and ranges of key thermodynamic parameters

Term	Value
Population size for JA	10, 20 and 30
Population size for GA	10, 20,30, 50 and 100
Generation of optimization	100
Geothermal water temperatures, ℃	150.00, 160.00 and 170.00
Flash pressure, kPa	50.00-600.00
Steam turbine back pressure, kPa	20.00-100.00
Ammonia mass fraction of basic solution, %	20.00-99.00
Ammonia-water turbine inlet pressure, kPa	1600.00-3500.00
Ammonia-water turbine backpressure, kPa	600.00-1500.00

Table 8 Optimization results

Term / η_{exg} / t_{geo}	Population size							
	JA			GA				
	10	20	30	10	20	30	50	100
150℃	23.57%	23.59%	23.59%	18.54%	21.28%	21.11%	23.12%	23.23%
160℃	25.05%	25.06%	25.06%	13.80%	23.58%	22.44%	24.47%	24.98%
170℃	26.25%	26.25%	26.25%	18.73%	25.24%	25.49%	26.03%	26.17%

Table 9 Results of thermoeconomic estimation under optimum performance condition

t_{geo} (℃)	$c_{P,tot}$ (\$/GJ)	$C_{P,tot}$ (\$/year)
150	1.69	8871.11
160	1.46	9267.67
170	1.33	10068.68

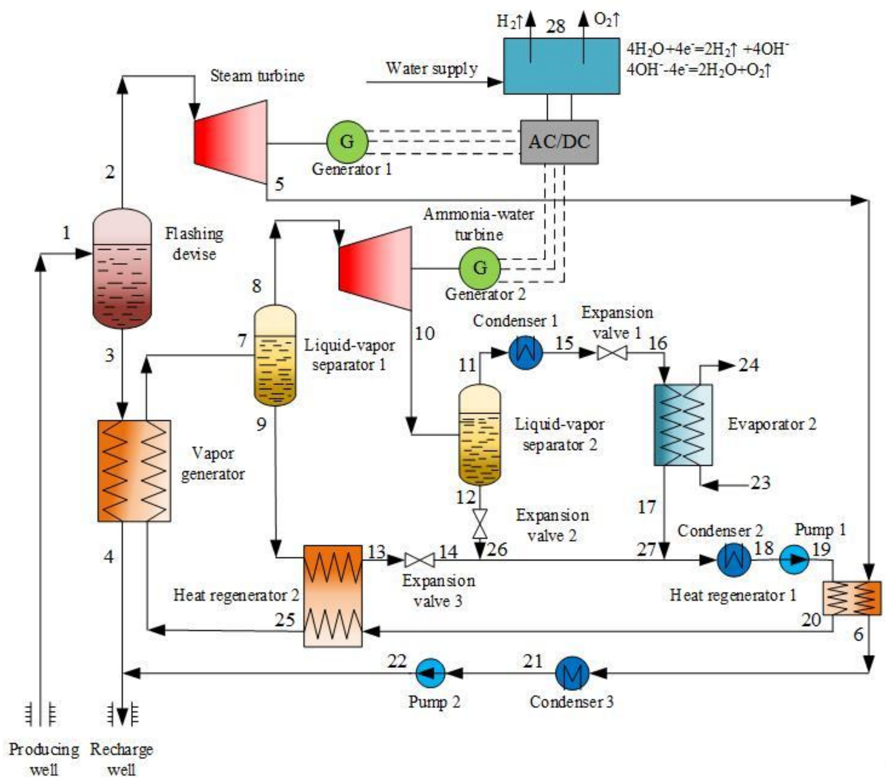

Fig. 1 The schematic diagram of a combined cooling and hydrogen production system

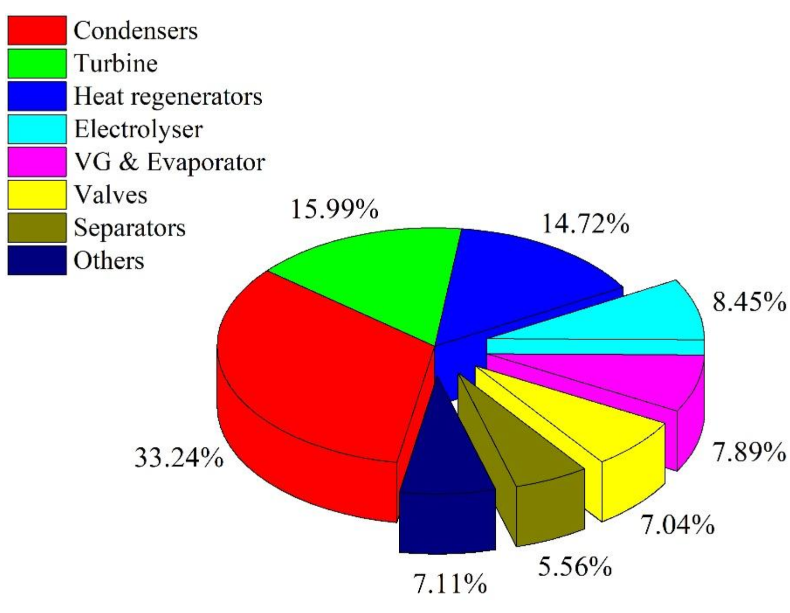

Fig. 2 Exergy destruction of different components

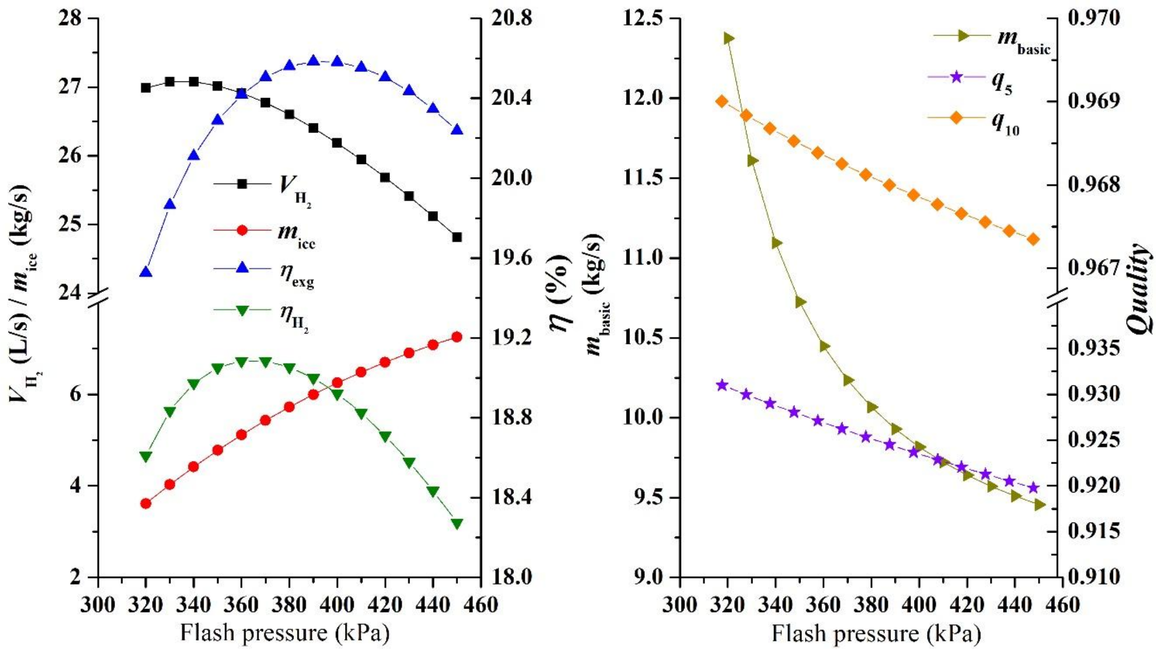

Fig. 3 The effect of flash pressure on system performance

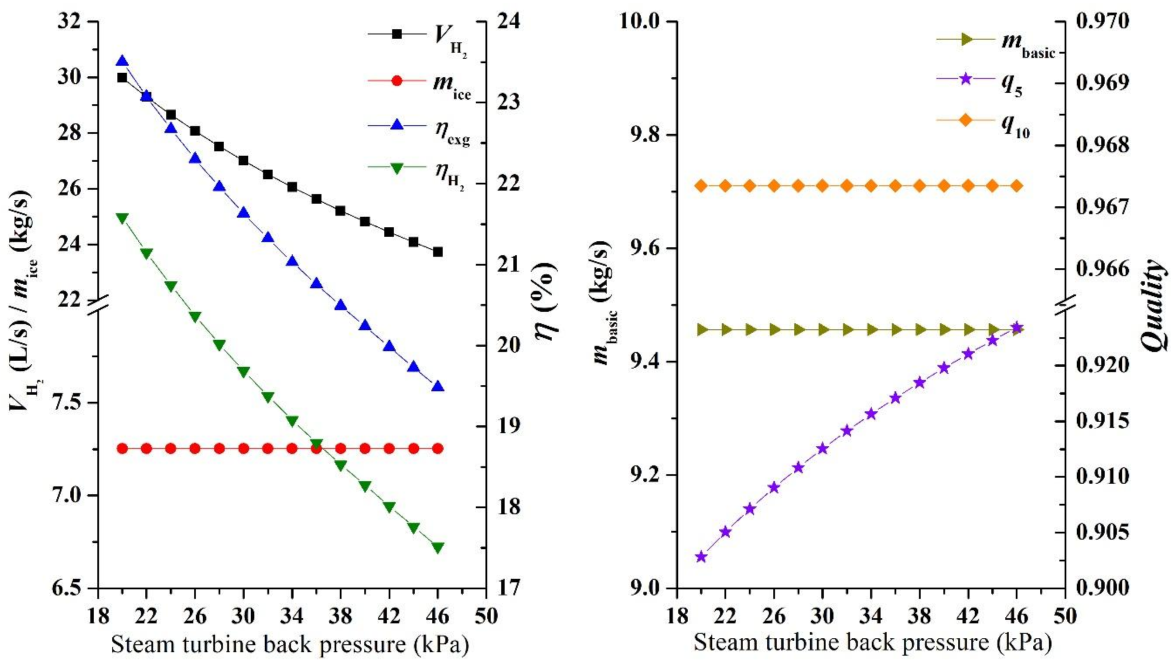

Fig. 4 The effect of steam turbine back pressure on the system performance

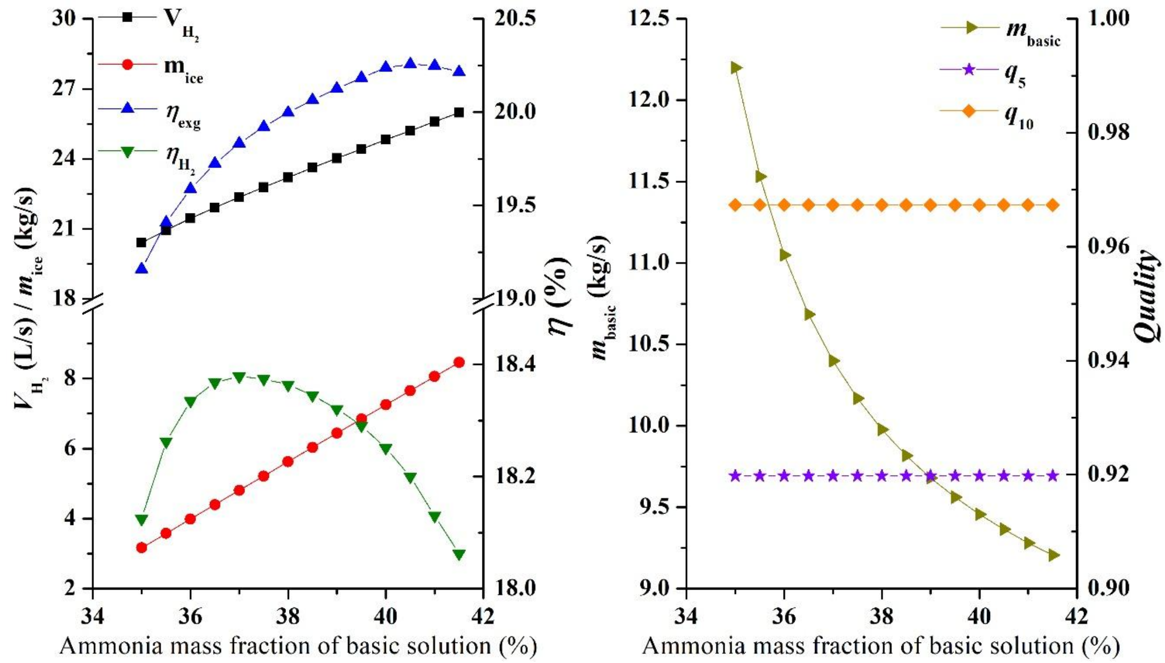

Fig. 5 The effect of ammonia mass fraction of basic solution on system performance

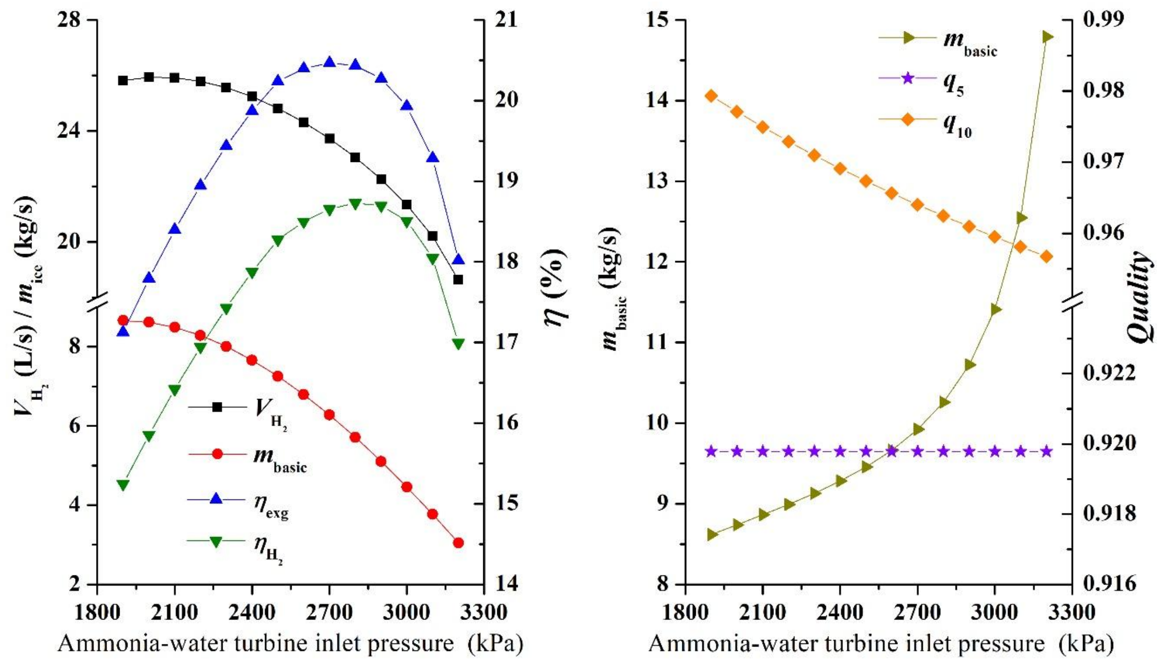

Fig. 6 The effect of ammonia-water turbine inlet pressure on system performance

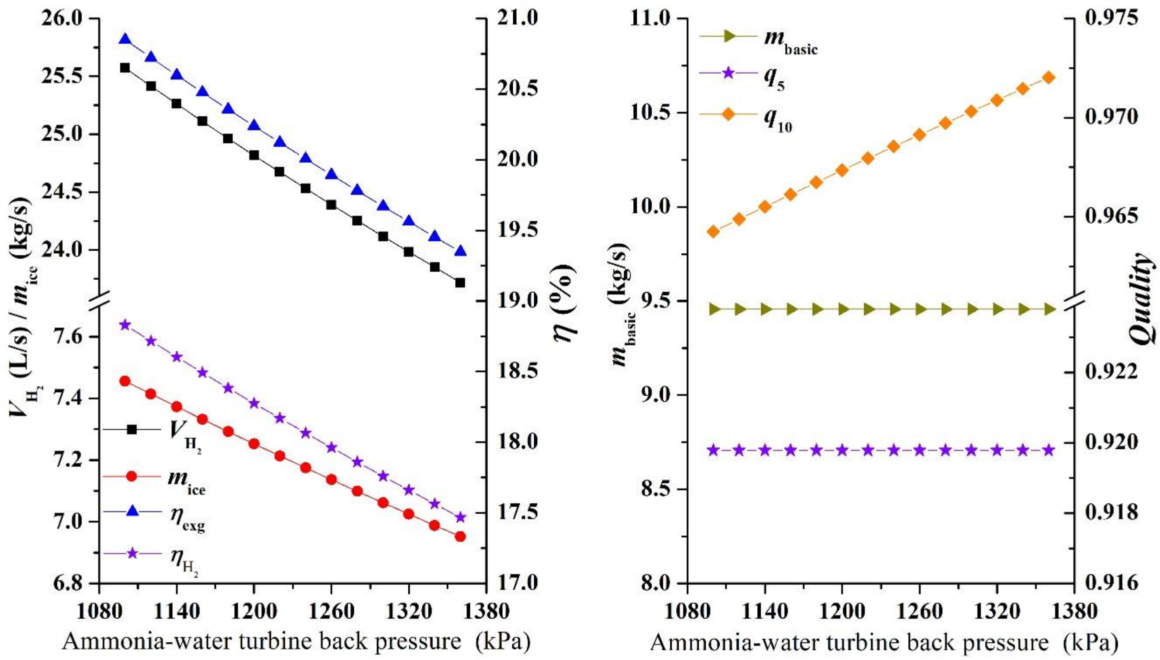

Fig. 7 The effect of ammonia-water turbine back pressure on system performance

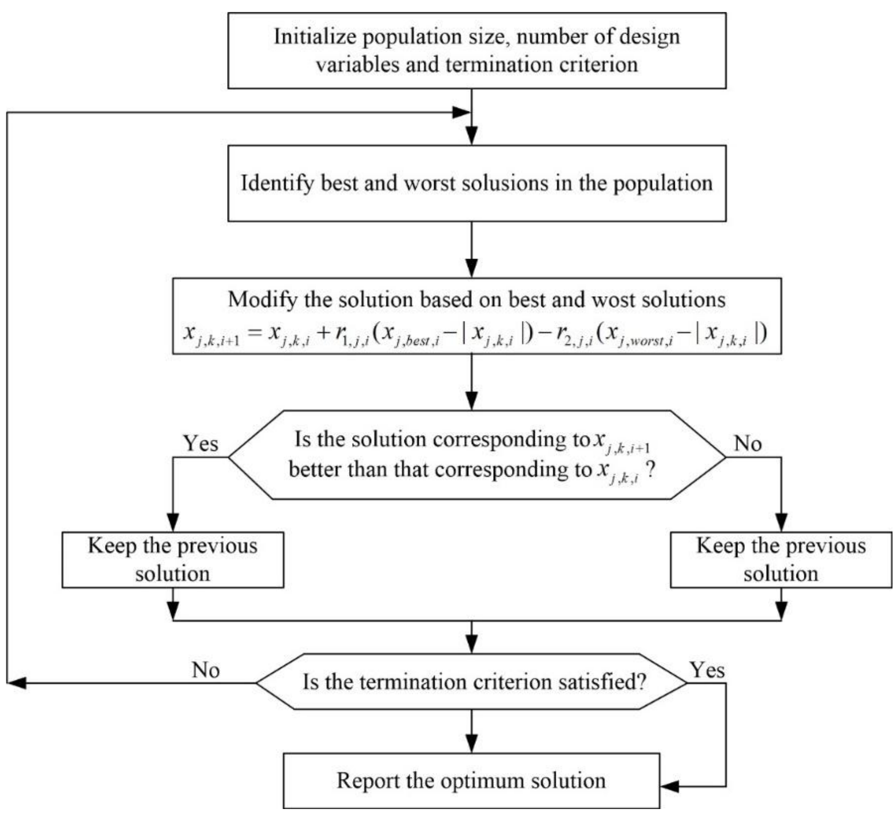

Fig. 8 The Flow chart of Jaya algorithm

Response to Reviewers

Dear editor & reviewers,

First of all, we would like to thank you very much for your second-round review of our paper and all your kind comments. These comments help us make better modifications and improve the quality of the paper. We have modified the manuscript accordingly in the revised manuscript. Please find below our responses and explanations for your comments and questions. All the modifications are highlighted in the manuscript.

Reviewers' comments:

Reviewer 1:

This is potentially an interesting paper. The proposed system combines a geothermal flash cycle, a Kalina cycle, ammonia water absorption refrigeration cycle and electrolyzer. The effect of operating parameters such as pressure and geothermal temperature on system performance are analyzed. The geothermal energy can be efficiently converted to storable hydrogen and ice. Based on mathematical model, some key parameters are analyzed to figure out their effect on the exergetic performance. I congratulate the author who took into consideration all my remarks and who has corrected the manuscripts according to our remarks by adding details. Therefore, according to the current state, the manuscript has become accretive to publish in the ECM. I ask the author to check the references cited in the manuscript.

Thank you for your recommendation. All references cited in the manuscript have been double checked.

Reviewer 2:

The authors replied well the comments which I have given. I think that the current version has a contribution to be publishable in ECM now.

Thank you for your recommendation.

Reviewer 3:

The author has revised this paper carefully. However, a major revision still required before it is acceptable. Please consider the following comments when you polish this manuscript.

1. Whether the mass flow rate of ammonia water through VG is a constant value or the pinch point temperature in the VG is constant?

In this paper, the pinch point temperature difference is a constant (10℃) as listed in Table 4. For given heat source, the mass flow rate of ammonia-water basic solution through VG varies with flash pressure, ammonia mass fraction of basic solution and ammonia-water turbine inlet pressure.

As the flash pressure increases, the mass flow rate of steam decreases while the mass flow of water separated from flashing device increases. As a result, it will provide more heat to bottom cycle and lead to an increase in mass flow rate of ammonia-water basic solution. When the ammonia mass fraction or the ammonia-water turbine inlet pressure increase, the specific enthalpy rise of basic solution increases significantly. This leads to a sight decease in mass flow rate of basic solution. As for the steam turbine back pressure and ammonia-water turbine back pressure, their variations don’t have any impact on the mass flow rate of ammonia-water basic solution. Therefore, the mass flow rate remains unchanged as back pressures vary.

To address reviewer’s concern, we have underlined the constant pinch point temperature difference and drawn curves to describe the variation of mass flow rate of ammonia-water basic solution in Figs. 3 to 7.

2. It's better to give the trend of some important parameters, such as the quality of turbine exhaust, the pinch point temperature in the VG and the cooling temperature in the evaporator.

As mention in previous response, the pinch point temperature difference is a constant (10℃) as listed in Table 4, while the mass flow rate of basic solution will vary with some key parameters. We have drawn curves to describe the variation of mass flow rate of ammonia-water basic solution and quality of turbine exhaust in Figs. 3 to 7. According to the engineering experience, the quality of turbine exhaust should not be lower than 0.88 [1]. The qualities of steam turbine exhaust and ammonia-water turbine exhaust are always higher than 0.88 as the five key parameters vary. In addition, the optimizations are also subject to this restriction.

To satisfy the requirement of ice-making, evaporating temperature and ice temperature are usually fixed values. The manufacturer of ice-maker OMT claims that the evaporating temperature should range from -8℃ to -20℃ [2]. Therefore, we fixed the evaporating temperature and ice temperature at -13℃ and -5℃ [3]. The evaporating temperature, ice temperature and relevant references have been added to the revised manuscript. Note that the key parameters have great impact on the mass flow rate of secondary ammonia-rich vapor. With fixed evaporating temperature and ice temperature, the mass flow rate of secondary ammonia-rich vapor will directly determine the refrigeration capacity and ice-making capacity. The variation of ice-making capacity are demonstrated in Figs. 3 to 7 and relevant discussions are presented in the manuscript.

[1] A. Ganjehkaviri, M.M. Jaafar, S. Hosseini. Optimization and the effect of steam turbine outlet quality on the output power of a combined cycle power plant. Energ Convers Manage. 89

(2015) 231-43.

[2] http://www.omt-icemachines.com/temperature-factors-of-ice-machine.html

[3] http://www.omt-icemachines.com/25t-flake-ice-machine.html

3. Why not give the exergy efficiency trend of the whole cycle when the main parameters change?

Actually, we've already demonstrate the system exergy efficiency (η_{exg}) in Figs. 3 to 7 and discussed its variation trend in the manuscript.

4. It would be easier for readers to understand if there is a table of point parameters of the whole cycle.

According to reviewer's comment, we have created a new table (Table 6) to demonstrate the thermodynamic parameters of each node under simulation condition.

5. In line 268, the word "since" cannot be used as an adverb. In line 320, there is a spelling mistake, it should be "low" rather than "law". Please check the grammatical and lexical errors again carefully.

The manuscript has been double checked and all grammatical and lexical errors have been modified.

Exergy Analysis and Optimization of a Combined Cooling and Power System Driven by Geothermal Energy for Ice-making and Hydrogen Production

Liyan Cao, Juwei Lou, Jiangfeng Wang*, Yiping Dai

Institute of Turbomachinery, Shaanxi Engineering Laboratory of Turbomachinery and Power Equipment, State Key Laboratory of Multiphase Flow in Power Engineering, School of Energy and Power Engineering, Xi'an Jiaotong University, Xi'an 710049, China

Corresponding author: Jiangfeng Wang.

Mailing address:

Institute of Turbomachinery, Shaanxi Engineering Laboratory of Turbomachinery and Power Equipment, State Key Laboratory of Multiphase Flow in Power Engineering,

School of Energy and Power Engineering

Xi'an Jiaotong University, Xi'an 710049, China

E-mail address: jfwang@mail.xjtu.edu.cn (JF Wang).

Exergy Analysis and Optimization of a Combined Cooling and Power System Driven by Geothermal Energy for Ice-making and Hydrogen Production

Liyan Cao, Juwei Lou, Jiangfeng Wang*, Yiping Dai

Institute of Turbomachinery, Shaanxi Engineering Laboratory of Turbomachinery and Power Equipment, State Key Laboratory of Multiphase Flow in Power Engineering, School of Energy and Power Engineering, Xi'an Jiaotong University, Xi'an 710049, China

Abstract

This paper investigates a combined cooling and power system driven by geothermal energy for ice-making and hydrogen production. The proposed system combines geothermal flash cycle, Kalina cycle, ammonia-water absorption refrigeration cycle and electrolyser. The geothermal energy can be efficiently converted to storable hydrogen and ice. Based on mathematical model, some key parameters are analyzed to figure out their effect on the exergetic performance. An exergy destruction for all components has been performed to find out the distribution of exergy inefficiency. The system exergetic efficiency is optimized by Jaya algorithm and Genetic algorithm and the optimization results are compared. According to the parametric analysis, the exergy efficiency decreases as the back pressure of steam turbine and the back pressure of ammonia-water turbine increase. The exergy efficiency could increase first and then decline, as flash pressure, ammonia-water turbine inlet pressure and ammonia mass fraction of basic solution increase. The optimization results show that the exergy efficiency reaches 23.59%, 25.06% and 26.25% when the geothermal water temperature is 150℃, 160℃ and 170℃. Jaya algorithm has highly precise optimization results.

Key words: Geothermal, Jaya algorithm, Hydrogen production, ice production

Nomenclature

C	cost rate ($\$\cdot year^{-1}$)
c	costs per unit of exergy ($\$\cdot J^{-1}$);
c_p	specific heat capacity, kJ/(kg K)
E	exergy, kW
HHV	higher heating value, kJ/mol
h	specific enthalpy, kJ/kg
I	exergy destruction, kW
M	molecular weight, g/mol
m	mass flow rate, kg/s
Q	energy, kW
q	quality
s	specific entropy, kJ/(kg K)
T	temperature, K
t	temperature, ℃
V	volumetric flow rate, L/s
VG	vapor generator
W	power, kW
W_y	annual power ($J\cdot year^{-1}$);
x	ammonia mass fraction, %
Z	annually levelized cost value ($\$\cdot year^{-1}$)

Greek letters

ρ	density, kg/m^3
η	efficiency, %
Subscript	
amb	ambient
awt	ammonia-water turbine
basic	ammonia-water basic solution
elec	electrolyser
exg	exergy
F	fuel
gen	generating
geo	geothermal water
H_2	hydrogen
ice	ice
in	inlet
l	liquid
mech	mechanical
motor	motor
net	net
P	product
poor	ammonia-poor solution
poor2	secondary ammonia-poor solution
pump	pump
ref	refrigeration

rich	ammonia-rich vapor
rich2	secondary ammonia-rich vapor
s	isentropic
st	steam turbine
tot	total
v	vapor
1-28	state point

1. Introduction

In recent years, the demand for fossil fuels increases dramatically, which has aroused great concerns about the environmental pollution, greenhouse gas emission and security of energy supply. Different countries have made plans to achieve diversification of energy supply and increase the proportion of renewable energy. Geothermal energy is one of reliable, sustainable and environmentally friendly renewable energy, which has drawn great attention.

Worldwide, geothermal power generation is the most common and efficient method for geothermal utilization. Geothermal power generation technologies in use mainly include flash cycle, binary cycle and flash-binary cycle. Researchers conducted analysis and optimization of the flash cycle [1-3]. The optimization results exhibited the optimum flash pressure to maximize the power output. But the flash cycle requires a relatively high geothermal water temperature. For the geothermal well with low water temperature, Kalina cycle [4-7] is regarded as reliable technologies, since Kalina cycle take full advantage of ammonia-water mixture. Owing to its low-boiling point and temperature slide character, ammonia-water mixture can achieve better thermal match in evaporator to reduce the irreversible loss. On this basis, Kalina cycle has applied as the bottom cycle of flash cycle to raise the thermal and exergy efficiency [8, 9]. The comparison results showed that flash-Kalina cycle generated more power than double-flash cycle did. However, the traditional flash cycle, Kalina cycle or flash-Kalina cycle only generate power, which cannot satisfy the diversified energy demand of users.

The cogeneration systems can supply users with different kinds of energy including electricity, heat and cooling, but more importantly, it has higher energy efficiency. From thermodynamic point of view, cooling is not an easily accessible energy compared to heat. It is usually converted from heat or electricity. Therefore, this brings a focus on the combined power and cooling (CCP) system employing ammonia–water as working fluid. Goswami and Xu [10, 11] came up with a CCP system based on ammonia-water absorption refrigeration cycle. They claimed that this system had potential for efficient recovery of low-grade heat source. Rashidi and Yoo [12] proposed a CCP system that combined the Kalina power cycle and the ejector absorption refrigeration cycle. They compared this new system with another CCP system and found the new system has higher refrigeration output and thermal efficiency. Shokati *et al*. [13] came up with a new CCP system. The proposed cycle was the combination of a Kalina cycle and an absorption refrigeration cycle. Han *et al*. [14] conducted experimental investigation on a combined refrigeration/power generation system. The net power output and cooling output were 1.02kW and 11.67 kW.

However, the energy demand may fluctuate with time. This will trigger the mismatch between energy supply and demand. For lower energy demand, the operation condition of CCP system can be adjusted to meet the change of energy demand, but CCP system will deviate from the design condition and go against the efficient operation. To solve this problem, some researchers try to store electricity energy into hydrogen energy to eliminate the energy mismatch problem. Yüksel [15] conducted thermodynamic analysis for a combined cooling, power and hydrogen production system driven by solar energy. The high temperature water from solar collector drove an Organic rankine cycle and an absorption cooling system to produce electricity and cooling, respectively. A part of electricity was used for hydrogen production by a Proton Exchange Membrane (PEM) electrolyser. Khanmohammadi *et al*. [16] proposed a similar combined cooling, power and hydrogen production system and carried out a parametric study to determine the main design parameters and their effects on the system performance. Akrami *et al*. [17] proposed multi-generation system comprised of a geothermal based organic Rankine cycle, domestic water heater, absorption refrigeration cycle and PEM electrolyser. The geothermal water was used to drive ORC and to heat the domestic water up, successively. A part of power generated by organic turbine was used for hydrogen production and organic turbine exhaust was used as the heat source of absorption refrigeration cycle. Yuksel *et al.* [18] came up with a novel integrated geothermal energy-based system for cooling and hydrogen production. The cooling and hydrogen was produced by an absorption refrigeration cycle and PEM electrolyser, separately. They claimed that the energetic and exergetic efficiencies of the integrated system could reach to 42.59% and 48.24%, respectively. Parham *et al*. [19] proposed a novel multi-generation system including an open absorption heat transformer, an ORC and an electrolyser for hydrogen production. They analyzed the system from both first and second laws of thermodynamics. Boyaghchi and Safari [20] proposed a new designed quadruple energy production system integrated with geothermal energy, which could produce electricity power, heating, cooling and hydrogen. They conducted thermoeconomic analysis and optimization for the system, and found that the total avoidable investment cost rate is improved within 17.4% relative to the base point. Ahmadi *et al*. [21] proposed a multigeneration energy system to produce power, heating, cooling, hot water and hydrogen. They performed multi-objective optimization for the system and determined the optimum thermoeconomic performance.

All the combined cooling, power and hydrogen systems could convert electricity to hydrogen that can be easily stored to counter the mismatch between supply and demand. However, these papers don't take the cooling mismatch into consideration. In addition, all the systems generate electricity and cooling with separate cycles, and different cycles run with different working medium. As a result, the systems have very complex configurations. We believe that the cogeneration system could have a more compact configuration and all the products are storable. Toward this end, we propose a combined cooling and power system driven by geothermal energy for ice-making and hydrogen production in this paper. The system consists of a top geothermal flash cycle, a bottom combined cooling and power cycle as well as an electrolyser. For the bottom cycle, both Kalina cycle and absorption refrigeration cycle can adopt ammonia-water as working fluid, we integrate Kalina cycle with absorption refrigeration cycle by sharing same key components to simplify the system configuration. And electricity and cooling are converted to storable hydrogen and ice, respectively. We also conduct a parametric analysis to study the effect of key parameters on system performance. In addition, we use a novel optimization algorithm named Jaya algorithm to optimize the systems and compare the Jaya algorithm with Genetic algorithm to verify its accuracy.

2. System description

Fig. 1 shows the schematic diagram of a combined cooling and power system for ice-making and hydrogen production. The high-temperature geothermal water is pumped from geothermal well to flashing devise in which the geothermal water is decompressed and partially becomes steam. The steam expands in steam turbine and the exhaust leaves turbine with low temperature and low pressure. The remaining water from flashing devise is used to vaporize the ammonia-water basic solution in vapor generator (VG), and then the water is mixed with steam turbine exhaust and delivered to recharge well. The vaporized ammonia-water basic solution is delivered to separator 1, in which it is separated into ammonia-rich vapor and ammonia-poor solution. After expanding in ammonia-water turbine to generate electrical power, the ammonia-water turbine exhaust is separated into secondary ammonia-rich vapor and secondary ammonia-poor solution in separator 2. The secondary ammonia-rich vapor is condensed and throttled down to generate cold energy in evaporator. The generated cold energy is used to produce ice. The secondary ammonia-poor solution from separator 2, the secondary ammonia-rich vapor from evaporator and the ammonia-poor solution from separator 1 are mixed and condensed into supercooling ammonia-water basic solution in condenser 2. The ammonia-water basic solution is preheated in regenerator 1 and regenerator 2. Finally, the ammonia-water basic solution is delivered to VG to complete the bottom cycle. All the power generated by turbines is given to electrolyser to break the molecules of water into hydrogen and oxygen.

3. Mathematical model and performance criteria

The mathematical model is established based on mass and energy conservation. To simplify the mathematical model, some assumptions are applied as follows:

(1) The system is simulated in steady state.

(2) The flows across the throttle valve are isenthalpic.

(3) The working fluid is condensed to saturated liquid in condenser.

(4) The pressure loss and heat loss are neglected.

(5) Turbines and pumps have isentropic efficiency.

3.1 Mathematical model

For the flashing devise, the mass and energy balance equations are described as:

$$\frac{m_{\mathrm{v}}}{m_{\mathrm{geo}}} = \frac{h_1 - h_3}{h_2 - h_3} \tag{1}$$

$$m_{\mathrm{geo}} = m_l + m_{\mathrm{v}} \tag{2}$$

For the VG, energy balance equation is expressed as:

$$m_{\mathrm{l}}(h_3 - h_4) = m_{\mathrm{basic}}(h_7 - h_9) \tag{3}$$

For the steam turbine, the isentropic expansion efficiency is represented as:

$$s_2 = s_{5\mathrm{s}} \tag{4}$$

$$\eta_{\mathrm{st}} = \frac{h_2 - h_5}{h_2 - h_{5\mathrm{s}}} \tag{5}$$

For the separator 1, the mass and energy balance equation are written as:

$$m_{\mathrm{basic}} = m_{\mathrm{rich}} + m_{\mathrm{poor}} \tag{6}$$

$$m_{\mathrm{basic}} x_7 = m_{\mathrm{rich}} x_8 + m_{\mathrm{poor}} x_9 \tag{7}$$

$$m_{\mathrm{basic}} h_7 = m_{\mathrm{rich}} h_8 + m_{\mathrm{poor}} h_9 \tag{8}$$

For the ammonia-water turbine, isentropic expansion efficiency can be expressed as:

$$s_8 = s_{10\mathrm{s}} \tag{9}$$

$$\eta_{\mathrm{awt}} = \frac{h_8 - h_{10}}{h_8 - h_{10\mathrm{s}}} \tag{10}$$

For the evaporator, the energy balance equation is given by:

$$m_{\mathrm{rich2}}(h_{17} - h_{16}) = m_{\mathrm{water}}(h_{23} - h_{24}) \tag{11}$$

For the heat regenerator 1, the energy balance equation is defined as:

$$m_{\mathrm{basic}}(h_{20} - h_{19}) = m_{\mathrm{v}}(h_5 - h_6) \tag{12}$$

For the heat regenerator 2, the energy balance equation is described as follows:

$$m_{\mathrm{basic}}(h_{25} - h_{20}) = m_{\mathrm{poor2}}(h_9 - h_{13}) \tag{13}$$

For the evaporator, the mass and energy balance equations are as follows:

$$m_{\mathrm{rich}} = m_{\mathrm{rich2}} + m_{\mathrm{poor2}} \tag{14}$$

$$m_{\mathrm{rich}} h_{10} = m_{\mathrm{rich2}} h_{11} + m_{\mathrm{poor2}} h_{12} \tag{15}$$

The isenthalpic flow across the throttle valves has the form:

$$h_{13} = h_{14} \tag{16}$$

$$h_{15} = h_{16} \tag{17}$$

$$h_{12} = h_{26} \tag{18}$$

The power consumption and isentropic efficiency of pumps are defined as:

$$\eta_{\mathrm{pump}} = \frac{h_{19\mathrm{s}} - h_{18}}{h_{19} - h_{18}} \tag{19}$$

$$\eta_{\mathrm{pump}} = \frac{h_{22\mathrm{s}} - h_{21}}{h_{22} - h_{21}} \tag{20}$$

$$W_{\mathrm{pump}} = (h_{19} - h_{18}) m_{\mathrm{basic}} + (h_{22} - h_{21}) m_{\mathrm{v}} \tag{21}$$

The electric power generated by turbine is given by:

$$W_{\mathrm{st}} = m_{\mathrm{v}}(h_2 - h_5) \tag{22}$$

$$W_{\mathrm{awt}} = \left[m_{\mathrm{rich}}(h_8 - h_{10}) \right] \tag{23}$$

$$W_{\mathrm{net}} = \left(W_{\mathrm{st}} + W_{\mathrm{awt}} \right) \eta_{\mathrm{mech}} \eta_{\mathrm{gen}} - W_{\mathrm{pump}} / \eta_{\mathrm{pump,motor}} \tag{24}$$

where η_{mech}, η_{gen} and $\eta_{\mathrm{pump,motor}}$ are mechanical efficiency, generator efficiency and pump motor efficiency, respectively.

In this paper, all the power is used to produce hydrogen by electrolysis. The Higher Heating Value (*HHV*) of hydrogen is 285.840 kJ/mol. That's to say, burning one mold of hydrogen would produce one mole of water and release 285.840kJ of heat. Ideally, electrolyzing one mole of water to produce one mole of hydrogen will consumes 285.840kJ of heat [22].

$$4\mathrm{H_2O}+4\mathrm{e}^- = 2\mathrm{H_2}\uparrow + 4\mathrm{OH}^- \tag{25}$$

$$4\mathrm{OH}^- - 4\mathrm{e}^- = 2\mathrm{H_2O} + \mathrm{O_2}\uparrow \tag{26}$$

In this paper, an alkaline electrolyser is chosen to produce hydrogen. The total efficiency of the electrolyser is 77%, which has taken energy dissipations of AC/DC converter and other equipment into consideration [22]. The hydrogen production is given by

$$V_{\mathrm{H_2}} = \frac{W_{\mathrm{net}} \cdot 1000 \cdot M_{\mathrm{H_2}} \cdot \eta_{\mathrm{elec}}}{HHV \cdot \mathrm{V}_{\mathrm{H_2}} \cdot \rho_{\mathrm{H_2}}} \tag{27}$$

where $V_{\mathrm{H_2}}$, $M_{\mathrm{H_2}}$, $\rho_{\mathrm{H_2}}$ and η_{elec} are volumetric flow rate of hydrogen, molecular weight of hydrogen, density of hydrogen and efficiency of the electrolyser, respectively.

The cold energy generated by evaporator to make ice is defined as:

$$Q_{\text{ref}} = m_{\text{ice}} c_{\text{p}} (T_{23} - T_{24}) \tag{28}$$

where m_{ice} is the ice production rate.

3.2 Performance criteria

The thermodynamic performance of system is evaluated by system exergy efficiency and hydrogen exergy efficiency. The exergy is given by:

$$E = (h - h_{\text{amb}}) - T_{\text{amb}}(s - s_{\text{amb}}) \tag{29}$$

The cold exergy is written as:

$$E_{\text{ref}} = T_{\text{amb}}(s - s_{\text{amb}}) - (h - h_{\text{amb}}) \tag{30}$$

The exergy of hydrogen approximately equals to the HHV of H_2, namely 285.840 kJ/mol [22].

The system exergy efficiency is expressed as:

$$\eta_{\text{exg}} = \frac{E_{\text{H}_2} + E_{\text{ref}}}{E_{\text{in}}} \tag{31}$$

The hydrogen efficiency is expressed as:

$$\eta_{\text{exg-H}_2} = \frac{E_{\text{H}_2}}{E_{\text{in}}} \tag{32}$$

E_{in} is the exergy input defined as:

$$E_{\text{in}} = m_{\text{geo}} E_1 - m_l E_4 - m_{\text{v}} E_{22} \tag{33}$$

The exergy destruction is defined as follows.

$$I = \Delta_{\text{out}}^{\text{in}} E \tag{34}$$

3.3. Mathematical model validation

Essentially, our proposed system is a combination of three cycles: a geothermal flash cycle, a Kalina cycle with a backpressure turbine and an absorption refrigeration cycle. To verify the feasibility of this combination, we conducted a mathematical model validation. Three parts of the proposed system are respectively validated with data in open literature [23-25]. Tables 1 to 3 demonstrate the validation results, and the simulation results are well consistent with the data in literature.

4. Results and discussion

In this section, a parametric analysis for the combined cooling and power system for ice-making and hydrogen production is performed. Some key parameters (e.g. flash pressure, ammonia mass fraction of basic solution, ammonia-water turbine inlet pressure, ammonia-water turbine back pressure, steam turbine back pressure) are analyzed to figure out their effect on the system performance. Note that the pinch point temperature difference is a constant. The thermodynamic properties of working fluid are calculated by REFPROP 9.1 developed by the National Institute of Standard and Technology (NIST) of the United States. The simulation of the system is conducted by MATLAB software. To ensure the operation safety, quality of turbine exhaust should not be lower than 0.88 [26]. All the analyses are subject to this restriction. To satisfy the requirement of ice-making, the evaporating temperature and ice temperature are -13℃[27] and -5℃[28], respectively.

The simulation boundary condition and simulation results are listed in Table 4 and Table 5. Table 6 demonstrates the thermodynamic parameters of each node under simulation condition. Fig. 2 illustrates the exergy destruction distribution of critical components under simulation condition.

Fig. 2 shows the exergy destruction of different components. The largest exergy destruction takes place in condensers, which is mainly caused by large heat transfer temperature differences. The exergy destruction of steam turbine and ammonia-water turbine are 15.99%. Heat regenerators contribute 14.72% of total exergy destruction. For VG & evaporator, valves, separators and other components, the exergy destruction is 7.89%, 7.04%, 5.56% and 7.11%, respectively.

4.1. Parametric analysis

Fig. 3 shows the effect of flash pressure on system performance. As the flash pressure increases, the mass flow rate of steam decreases, leading to a decrease in the power output of steam turbine. Meanwhile, the mass flow rate of water from flashing device increases with flash pressure. As a result, it will provide more heat to bottom cycle and lead to an increase in mass flow rate of ammonia-water basic solution. The mass flow rate of ammonia-rich vapor and the power output of ammonia-water turbine increase as well. Under the comprehensive impact of steam turbine and ammonia-water turbine, the net power output of the system firstly increases and then decreases. Thus, the hydrogen production has the same variation with net power output when the flash pressure increases. The increment of the mass flow rate of secondary ammonia-rich vapor results in the increase in refrigeration exergy. Therefore, the ice production increases. Note that the hydrogen production increases firstly and then decreases, the variation of hydrogen exergy efficiency also shows a convex curve. According to Eq. (31), system exergy efficiency is determined by hydrogen exergy, refrigeration exergy and total exergy input. Note that the refrigeration exergy is negligibly small and has little impact on exergy efficiency comparing with hydrogen exergy. As a result, the variation of system exergy efficiency is also a convex curve. Note that q_5 and q_{10} refer to the qualities of steam turbine exhaust and ammonia-water turbine exhaust. The qualities are both higher than 0.88. It won’t cause severe erosion of turbine blades.

Fig. 4 shows the effect of steam turbine back pressure on the system performance. Note that the bottom cycle is independent of the steam turbine back pressure, the mass flow rate of ammonia-water basic solution, the power output of ammonia-water turbine, the refrigeration exergy and ice production won't change with variation of the steam turbine back pressure. Meanwhile, the increment of steam turbine back pressure causes a decrease in power output of steam turbine. Consequently, the decreasing net power output of the system results in the decreasing hydrogen production of the system. The hydrogen exergy efficiency and system exergy efficiency decrease as well. The qualities of steam turbine exhaust and ammonia-water turbine exhaust are higher than 0.88 when steam turbine back pressure varies.

Fig. 5 shows the effect of ammonia mass fraction of basic solution on system performance. When the ammonia mass fraction of basic solution increases, the power output of steam turbine remains unchanged and the mass flow rate of ammonia-rich vapor and secondary ammonia-rich vapor rise simultaneously, which enables the net power output, the hydrogen production, the refrigeration exergy and ice production increase, simultaneously. Meanwhile, the energy and exergy input increase with ammonia mass fraction of basic solution significantly. According to Eq. (31) and (32), the hydrogen exergy efficiency and system exergy efficiency both show the convex curves under the combined impact of increasing exergy input, hydrogen production and refrigeration exergy. The qualities of steam turbine exhaust and ammonia-water turbine exhaust lie in safety zone.

Fig. 6 shows the effect of ammonia-water turbine inlet pressure on system performance. The flash cycle is independent of ammonia-water turbine inlet pressure.

Thus, the power output of steam turbine remains unchanged. When the ammonia-water turbine inlet pressure increases, the variation of the specific enthalpy drop in ammonia-water turbine is opposite to that of the mass flow rate of ammonia-rich vapor. Under the impact of these two factors, the net power output of the system as well as the hydrogen production firstly increases and then decreases. In addition, the mass flow rate of secondary ammonia-rich vapor decrease, which causes a decrease in refrigeration exergy and ice production. Comparing with hydrogen exergy, the impact of refrigeration exergy on system exergy efficiency is negligibly small. Dominated by hydrogen exergy, both hydrogen exergy efficiency and system exergy efficiency increase first and then decrease. The qualities of steam turbine exhaust and ammonia-water turbine exhaust won't cause severe erosion of turbine blades.

Fig. 7 shows the effect of ammonia-water turbine back pressure on system performance. As the ammonia-water turbine back pressure increases, the mass flow rates of basic solution and ammonia-rich vapor remain unchanged, and the enthalpy drop through ammonia-water turbine decreases. This causes a decrease in power output of ammonia-water turbine. Meanwhile, the power output of steam turbine keeps unchanged. Therefore, the net power output of the system decreases, which leads to the decline of hydrogen production. The refrigeration exergy and ice production decrease since the mass flow rate of secondary ammonia-rich solution decreases. Influenced by the decrease in hydrogen exergy and refrigeration exergy, the hydrogen exergy efficiency and system exergy efficiency decline. The qualities of steam turbine exhaust and ammonia-water turbine exhaust are acceptable.

4.2. Optimization

According to the parametric analysis, there may be an optimum performance for the combined cooling and power system driven by geothermal energy for ice-making and hydrogen production. Thus, a performance optimization is conducted to obtain the maximum system exergy efficiency. There are many optimization methods, such as Genetic algorithm (GA), Teaching-learning-based optimization (TLBO), Evolution Strategy (GE) and Evolution Programming (EP). For the performance optimization of the system driven by low temperature heat source, GA is the most commonly used optimization method for its global optimization ability [29-31].

Recently, Rao and Waghmare [32] proposed a new optimization algorithm named Jaya algorithm (JA). Unlike other algorithms, JA requires only the common control parameters such as population size, number of generations and elite size to run the optimization algorithm. And other algorithms require common control parameters as well as their own algorithm-specific parameters, which could add complexity to the algorithms [32]. The author tested JA and other several optimization algorithms on 21 benchmark problems related to constrained design optimization and claimed that JA could get highly precise optimization results with less computational time. The brief introduction of JA is as follows.

The objective function $f(x)$, which is a function of m design variables (j=1,2,…,m), is to be maximized and minimized by JA. At any i^{th} generation, there are n candidate solutions associated with n populations (k=1,2,…,n). And $x_{j,k,i}$ is the j^{th} variable in k^{th} population at i^{th} generation. The best value and worst value among n candidate solutions at i^{th} generation are $f(x)_{best,i}$ and $f(x)_{worst,i}$. Therefore, $x_{j,best,i}$ is the j^{th} variable in the population that corresponds to the best candidate solution $f(x)_{best,i}$, and $x_{j,worst,i}$ is the j^{th} variable in the population that corresponds to the worst candidate solution $f(x)_{worst,i}$ at i^{th} generation. For $(i+1)^{th}$ generation, x is modified as,

$$x_{j,k,i+1} = x_{j,k,i} + r_{1,j,i}(x_{j,best,i} - |x_{j,k,i}|) - r_{2,j,i}(x_{j,worst,i} - |x_{j,k,i}|) \tag{35}$$

where $r_{1,j,i}$ and $r_{2,j,i}$ both are the random numbers between 0 and 1. The Flow chart of Jaya algorithm is showed in Fig. 8.

To verify the optimization accuracy of JA algorithm, a system performance optimization is conducted by using both JA and GA with the same boundary condition and common control parameters. It is noted that the system is optimized under three different geothermal water temperatures (150 ℃, 160 ℃ and 170 ℃) to guarantee reliability of results. For each geothermal water temperature, the optimizations with JA and GA are performed with three and five different population size, respectively. The optimization with JA is carried out using the program written in Matlab by authors. The optimization with GA is performed by Matlab optimization tool box. All optimizations are running in the completely same computing environment. The operation parameters of optimization algorithm and ranges of key thermodynamic parameters are listed in Table 7 and the optimization results are listed in Table 8.

For each geothermal water temperature, the optimum exergy efficiencies calculated by JA are the same under three different population sizes. The exergy efficiencies are 23.59%, 25.06% and 26.25% when geothermal water temperatures are 150℃, 160℃ and 170℃. These results are almost equal to those calculated by GA with population sizes of 50 and 100. Note that small population size leads to inaccurate results of GA. That's to say, JA gets accurate results with less population and has potential to save computational time.

To verify the thermoeconomic feasibility, we have conducted thermoeconomic estimation for the proposed system under optimum performance conditions. In this paper, all exchangers are plate heat exchangers (PHE) and separators are vertical cyclone type. The heat transfer correlations and size estimation model for PHEs and separators are demonstrated in Ref. [33]. The *module costing technique* [34] is used to estimate the equipment costs, and the *exergy costing approach* [34] is applied to calculate the cost of product. We assume the lifespan (n) and annual working hours (t_y) of the proposed system are 25 years and 4000 hours, respectively. The annual cost balance is given by

$$C_{\mathrm{P,tot}} = C_{\mathrm{F,tot}} + Z_{\mathrm{tot}}$$

where $C_{\mathrm{P,tot}}$ is annual product cost rate, $C_{\mathrm{F,tot}}$ is annual fuel cost rate, Z_{tot} is the annually levelized cost of equipment. The annual product cost per unit of exergy output is expressed as

$$c_{\mathrm{P,tot}} = \frac{C_{\mathrm{P,tot}}}{E_{\mathrm{P,tot}}} = \frac{C_{\mathrm{P,tot}}}{W_{\mathrm{y,net}} + E_{\mathrm{y,ref}}}$$

where the $W_{\mathrm{y,net}}$ is the annual net power output and $E_{\mathrm{y,ref}}$ is the annual cold exergy output.

$$E_{\mathrm{y,ref}} = E_{\mathrm{ref}} \cdot 3600 \cdot t_{\mathrm{y}}$$

$$W_{\mathrm{y,net}} = W_{\mathrm{net}} \cdot 3600 \cdot t_{\mathrm{y}}$$

The specific thermoeconomic models are demonstrated in Ref. [35]. Table 9 shows the results of thermoeconomic estimation under optimum performance condition.

As the temperature of geothermal water increases, the annual product cost rate increases and the annual product cost per unit of exergy output decreases.

5. Conclusions

In this paper, we propose a combined ice-making and hydrogen production system. We investigate the exergy destruction of different components and analyze the effect of key parameters on system performance. We also conduct an optimization with JA and GA to search for maximum exergy efficiencies under three different geothermal water temperatures. The main conclusions are as follow:

(1) The condensers contribute most to the exergy destruction owing to the high temperature difference. The exergy efficiency decreases as back pressure of steam turbine and ammonia-water turbine increase. And exergy efficiency shows a convex curve, as flash pressure, ammonia-water turbine inlet pressure and ammonia mass fraction of basic solution increase.

(2) The optimum exergy efficiencies calculated by JA are about 23.59%, 25.06% and 26.25% for geothermal water temperature of 150℃, 160℃ and 170℃, respectively. JA could get highly precise optimization results with less population size.

Acknowledgements

The authors gratefully acknowledge the financial support by the National Natural Science Foundation of China (Grant No. 51476121).

References

[1] S. Amiri, H. Shokouhmand, A. Kahrobaian, S. Amiri. Optimum flashing pressure in single and double flash geothermal power plants. ASME 2008 Heat Transfer Summer Conference collocated with the Fluids Engineering, Energy Sustainability,

and 3rd Energy Nanotechnology Conferences. American Society of Mechanical Engineers2008. pp. 125-9.

[2] Y. Cerci. Performance evaluation of a single-flash geothermal power plant in Denizli, Turkey. Energy. 28 (2003) 27-35.

[3] N.A. Pambudi, R. Itoi, S. Jalilinasrabady, K. Jaelani. Exergy analysis and optimization of Dieng single-flash geothermal power plant. Energ Convers Manage. 78 (2014) 405-11.

[4] M. Fallah, S.M.S. Mahmoudi, M. Yari, R.A. Ghiasi. Advanced exergy analysis of the Kalina cycle applied for low temperature enhanced geothermal system. Energ Convers Manage. 108 (2016) 190-201.

[5] D. Fiaschi, G. Manfrida, E. Rogai, L. Talluri. Exergoeconomic analysis and comparison between ORC and Kalina cycles to exploit low and medium-high temperature heat from two different geothermal sites. Energ Convers Manage. 154 (2017) 503-16.

[6] E. Wang, Z. Yu, F. Zhang. Investigation on efficiency improvement of a Kalina cycle by sliding condensation pressure method. Energ Convers Manage. 151 (2017) 123-35.

[7] H. Saffari, S. Sadeghi, M. Khoshzat, P. Mehregan. Thermodynamic analysis and optimization of a geothermal Kalina cycle system using Artificial Bee Colony algorithm. Renew Energ. 89 (2016) 154-67.

[8] L. Cao, J. Wang, P. Zhao, Y. Dai. Thermodynamic comparison among double-flash flash-Kalina and flash-ORC geothermal power plants. International Journal of Thermodynamics. 19 (2016) 53-60.

[9] J. Wang, J. Wang, Y. Dai, P. Zhao. Thermodynamic analysis and optimization of a flash-binary geothermal power generation system. Geothermics. 55 (2015) 69-77.

[10] D.Y. Goswami, F. Xu. Analysis of a new thermodynamic cycle for combined power and cooling using low and mid temperature solar collectors. Journal of Solar Energy Engineering. 121 (1999) 91-7.

[11] F. Xu, D.Y. Goswami, S.S. Bhagwat. A combined power/cooling cycle. Energy. 25 (2000) 233-46.

[12] J. Rashidi, C. Yoo. A novel Kalina power-cooling cycle with an ejector absorption refrigeration cycle: Thermodynamic modelling and pinch analysis. Energ Convers Manage. 162 (2018) 225-38.

[13] N. Shokati, F. Ranjbar, M. Yari. A comprehensive exergoeconomic analysis of absorption power and cooling cogeneration cycles based on Kalina, part 1: Simulation. Energ Convers Manage. 158 (2018) 437-59.

[14] W. Han, Q. Chen, L. Sun, S. Ma, T. Zhao, D. Zheng, et al. Experimental studies on a combined refrigeration/power generation system activated by low-grade heat. Energy. 74 (2014) 59-66.

[15] Y.E. Yüksel. Thermodynamic assessment of modified Organic Rankine Cycle integrated with parabolic trough collector for hydrogen production. International Journal of Hydrogen Energy. (2017).

[16] S. Khanmohammadi, P. Heidarnejad, N. Javani, H. Ganjehsarabi. Exergoeconomic analysis and multi objective optimization of a solar based integrated energy system for hydrogen production. international journal of hydrogen energy. 42 (2017) 21443-53.

[17] E. Akrami, I. Khazaee, A. Gholami. Comprehensive analysis of a multi-generation energy system by using an energy-exergy methodology for hot water, cooling, power and hydrogen production. Applied Thermal Engineering. 129 (2018) 995-1001.

[18] Y.E. Yuksel, M. Ozturk, I. Dincer. Thermodynamic analysis and assessment of a novel integrated geothermal energy-based system for hydrogen production and storage. International Journal of Hydrogen Energy. (2017).

[19] K. Parham, H. Alimoradiyan, M. Assadi. Energy, exergy and environmental analysis of a novel combined system producing power, water and hydrogen. Energy. 134 (2017) 882-92.

[20] F.A. Boyaghchi, H. Safari. Parametric study and multi-criteria optimization of total exergetic and cost rates improvement potentials of a new geothermal based quadruple energy system. Energ Convers Manage. 137 (2017) 130-41.

[21] P. Ahmadi, I. Dincer, M.A. Rosen. Thermodynamic modeling and multi-objective evolutionary-based optimization of a new multigeneration energy system. Energ Convers Manage. 76 (2013) 282-300.

[22] Z.X. Sun, J.F. Wang, Y.P. Dai, J.H. Wang. Exergy analysis and optimization of a hydrogen production process by a solar-liquefied natural gas hybrid driven transcritical CO2 power cycle. International Journal of Hydrogen Energy. 37 (2012) 18731-9.

[23] A. Mohammadi, M. Mehrpooya. Energy and exergy analyses of a combined desalination and CCHP system driven by geothermal energy. Applied Thermal Engineering. 116 (2017) 685-94.

[24] A.D. Pasek, T.F. Soelaiman, C. Gunawan. Thermodynamics study of flash–binary cycle in geothermal power plant. Renewable and sustainable energy reviews. 15 (2011) 5218-23.

[25] H. Rostamzadeh, H. Ghaebi, T. Parikhani. Thermodynamic and thermoeconomic analysis of a novel combined cooling and power (CCP) cycle. Applied Thermal Engineering. 139 (2018) 474-87.

[26] A. Ganjehkaviri, M.M. Jaafar, S. Hosseini. Optimization and the effect of steam turbine outlet quality on the output power of a combined cycle power plant. Energ Convers Manage. 89 (2015) 231-43.

[27] http://www.omt-icemachines.com/temperature-factors-of-ice-machine.html.

[28] http://www.omt-icemachines.com/25t-flake-ice-machine.html.

[29] H.M. Hettiarachchi, M. Golubovic, W.M. Worek, Y. Ikegami. Optimum design criteria for an organic Rankine cycle using low-temperature geothermal heat sources. Energy. 32 (2007) 1698-706.

[30] S. Quoilin, M. Van Den Broek, S. Declaye, P. Dewallef, V. Lemort. Techno-economic survey of Organic Rankine Cycle (ORC) systems. Renewable and Sustainable Energy Reviews. 22 (2013) 168-86.

[31] D. Wei, X. Lu, Z. Lu, J. Gu. Performance analysis and optimization of organic Rankine cycle (ORC) for waste heat recovery. Energ Convers Manage. 48 (2007) 1113-9.

[32] R.V. Rao, G. Waghmare. A new optimization algorithm for solving complex constrained design optimization problems. Engineering Optimization. 49 (2017) 60-83.

[33] L. Cao, J. Wang, L. Chen, Y. Dai. Comprehensive analysis and optimization of Kalina-Flash cycles for low-grade heat source. Applied Thermal Engineering. 131 (2018) 540-52.

[34] R. Turton. Analysis, synthesis, and design of chemical processes. 4th ed. Prentice Hall, Upper Saddle River, NJ, 2012.

[35] Y. Zhao, J. Wang, L. Cao, Y. Wang. Comprehensive analysis and parametric optimization of a CCP (combined cooling and power) system driven by geothermal source. Energy. 97 (2016) 470-87.

Figure captions

Fig. 1 The schematic diagram of a combined cooling and hydrogen production system

Fig. 2 Exergy destruction of different components

Fig. 3 The effect of flash pressure on system performance

Fig. 4 The effect of steam turbine back pressure on the system performance

Fig. 5 The effect of ammonia mass fraction of basic solution on system performance

Fig. 6 The effect of ammonia-water turbine inlet pressure on system performance

Fig. 7 The effect of ammonia-water turbine back pressure on system performance

Fig. 8 The Flow chart of Jaya algorithm

Table 1 Mathematical model validation for flash cycle; (a) Present work, (b) Ref. [24].

State	*t* (℃)		*P* (kPa)		*m* (kg/s)	
	(a)	(b)	(a)	(b)	(a)	(b)
1	170.00	170.00	901.30	901.30	111.10	111.10
2	158.82	158.90	600.00	600.00	2.60	2.73
3	158.82	158.90	600.00	600.00	108.50	108.37
5	76.52	76.69	41.30	41.30	2.60	2.73

Table 2 Mathematical model validation for Kalina cycle with backpressure turbine; (a) Present work, (b) Ref. [25].

State	*t* (℃)		*P* (kPa)		*m* (kg/s)		*x* (%)	
	(a)	(b)	(a)	(b)	(a)	(b)	(a)	(b)
7	199.95	199.95	2000.00	2000.00	0.77	0.77	15.00	15.00
8	199.95	199.95	2000.00	2000.00	0.45	0.43	22.23	23.20
9	199.95	199.95	2000.00	2000.00	0.32	0.34	4.48	4.70
10	177.86	177.85	1235.00	1235.00	0.45	0.43	22.23	23.20

Table 3 Mathematical model validation for absorption refrigeration cycle; (a) Present work, (b) Ref. [23].

State	*t* (°C)		*P* (kPa)		*m* (kg/s)		*x* (%)	
	(a)	(b)	(a)	(b)	(a)	(b)	(a)	(b)
10	126.91	126.91	700.00	700.00	0.1440	0.1440	67.00	67.00
11	126.91	126.91	700.00	700.00	0.1429	0.1420	67.41	68.00
12	126.91	126.91	700.00	700.00	0.0011	0.0020	13.24	14.00
15	29.03	28.61	700.00	700.00	0.1429	0.1420	67.41	68.00
16	-3.02	-3.28	200.00	200.00	0.1429	0.1420	67.41	68.00
17	10.00	10.00	200.00	200.00	0.1429	0.1420	67.41	68.00
26	92.54	92.18	200.00	200.00	0.0011	0.0020	13.24	14.00

Table 4 Simulation conditions of system

Term	Value
Environment pressure (kPa)	101.33
Environment temperature (℃)	20.00
Geothermal water temperature (℃)	170.00
Geothermal water mass flow ($kg{\cdot}s^{-1}$)	30.00
Pinch point temperature difference (℃)	10.00
Approach point temperature difference (℃)	7.00
Evaporating temperature (℃) [27]	-13.00
Ice temperature (℃) [28]	-5.00
Turbine isentropic efficiency (%)	75.00
Pump isentropic efficiency (%)	65.00
Mechanical efficiency (%)	96.00
Generating efficiency (%)	95.00
Pump motor efficiency (%)	95.00
Alkaline electrolyser total efficiency (%)	77.00
Flash pressure (kPa)	450.00
Steam turbine back pressure (kPa)	30.00
Ammonia mass fraction of basic solution (%)	40.00
Ammonia-water turbine inlet pressure (kPa)	2500.00
Ammonia-water turbine back pressure (kPa)	1200.00

Table 5 System performance

Term	Value
Power of steam turbine (kW)	363.56
Power of ammonia-water turbine (kW)	110.83
Quality of steam turbine exhaust	0.92
Quality of ammonia-water turbine exhaust	0.97
Power consumption of pumps (kW)	60.28
Net power output (kW)	414.10
Hydrogen production (L/s)	24.82
Refrigeration capacity (kW)	837.66
Refrigeration exergy (kW)	34.25
Ice-making capacity (kg/s)	7.25
Hydrogen production exergy efficiency (%)	18.28
System exergy efficiency (%)	20.24

Table 6 Thermodynamic parameters of each node under simulation condition

State	t (℃)	P (kPa)	x (%)	h (kJ·kg^{-1})	m (kg·s^{-1})	quality
1	170.00	1000.00	0.00	719.20	30.00	0.00
2	147.90	450.00	0.00	2743.39	1.36	1.00
3	147.90	450.00	0.00	623.14	28.64	0.00
4	127.38	450.00	0.00	535.35	28.64	0.00
5	69.10	30.00	0.00	2420.31	1.36	0.91
6	69.10	30.00	0.00	1480.17	1.36	0.51
7	139.90	2500.00	40.00	728.54	9.46	0.13
8	139.90	2500.00	88.60	1964.55	1.27	1.00
9	139.90	2500.00	32.44	536.34	8.19	0.00
10	111.38	1200.00	88.60	1869.07	1.27	0.97
11	111.38	1200.00	90.60	1918.81	1.23	1.00
12	111.38	1200.00	29.27	395.09	0.04	0.00
13	69.10	2500.00	32.44	200.70	8.19	0.00
14	51.41	228.32	32.44	200.70	8.19	0.05
15	34.40	1200.00	90.60	400.15	1.23	0.00
16	-13.00	228.32	90.60	400.15	1.23	0.17
17	-6.00	228.32	90.60	1080.57	1.23	0.67
18	31.08	228.32	40.00	32.97	9.46	0.00
19	31.57	2500.00	40.00	37.06	9.46	0.00
20	61.10	2500.00	40.00	172.18	9.46	0.00

21	69.10	30.00	0.00	289.27	1.36	0.00
22	69.17	450.00	0.00	289.93	1.36	0.00
23	12.00	101.32	0.00	50.51	7.25	0.00
24	-5.00	101.32	0.00	21.12	7.25	0.00
25	121.76	2500.00	40.00	462.65	9.46	0.00
26	67.99	228.32	29.27	395.09	0.04	0.12
27	47.01	228.32	40.00	316.10	9.46	0.13

537

Table 7 Operation parameters of optimization algorithm and ranges of key thermodynamic parameters

Term	Value
Population size for JA	10, 20 and 30
Population size for GA	10, 20,30, 50 and 100
Generation of optimization	100
Geothermal water temperatures, ℃	150.00, 160.00 and 170.00
Flash pressure, kPa	50.00-600.00
Steam turbine back pressure, kPa	20.00-100.00
Ammonia mass fraction of basic solution, %	20.00-99.00
Ammonia-water turbine inlet pressure, kPa	1600.00-3500.00
Ammonia-water turbine backpressure, kPa	600.00-1500.00

Table 8 Optimization results

Term / η_{exg} / t_{geo}	Population size							
	JA			GA				
	10	20	30	10	20	30	50	100
150℃	23.57%	23.59%	23.59%	18.54%	21.28%	21.11%	23.12%	23.23%
160℃	25.05%	25.06%	25.06%	13.80%	23.58%	22.44%	24.47%	24.98%
170℃	26.25%	26.25%	26.25%	18.73%	25.24%	25.49%	26.03%	26.17%

Table 9 Results of thermoeconomic estimation under optimum performance condition

t_{geo} (℃)	$c_{P,tot}$ (\$/GJ)	$C_{P,tot}$ (\$/year)
150	1.69	8871.11
160	1.46	9267.67
170	1.33	10068.68

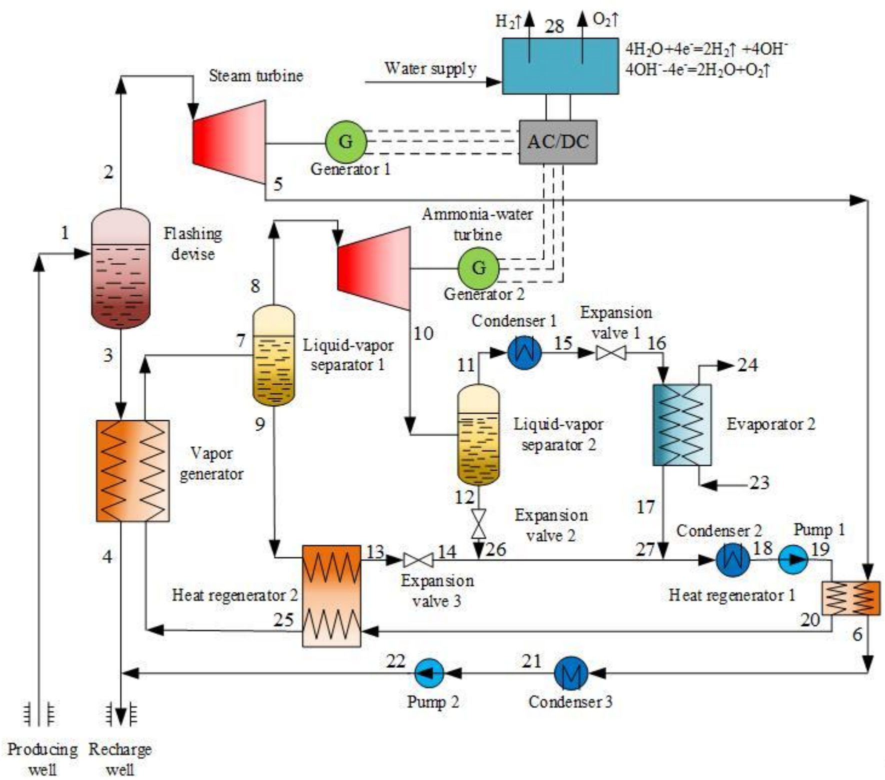

Fig. 1 The schematic diagram of a combined cooling and hydrogen production system

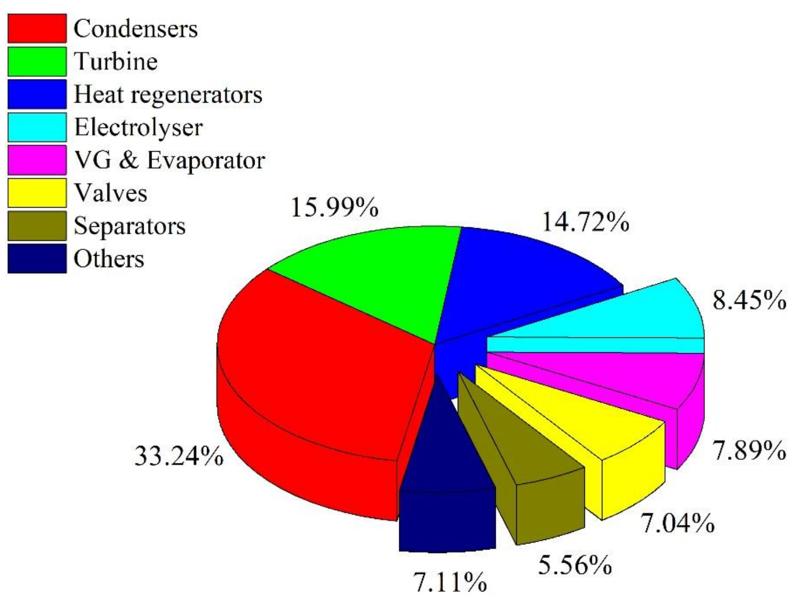

Fig. 2 Exergy destruction of different components

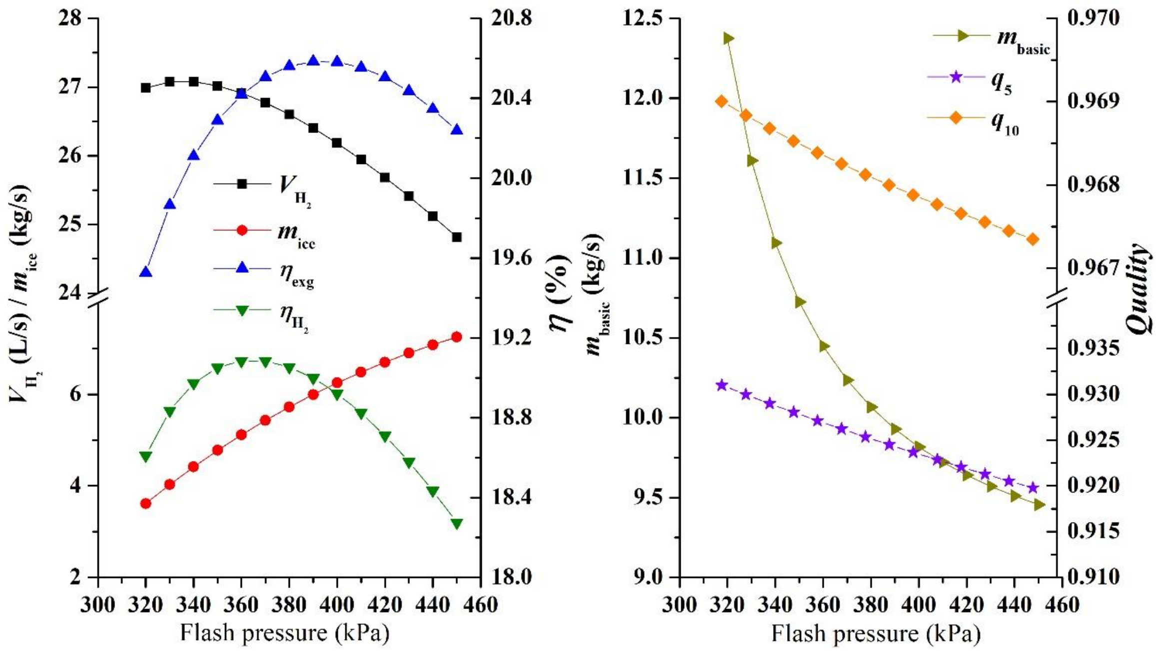

Fig. 3 The effect of flash pressure on system performance

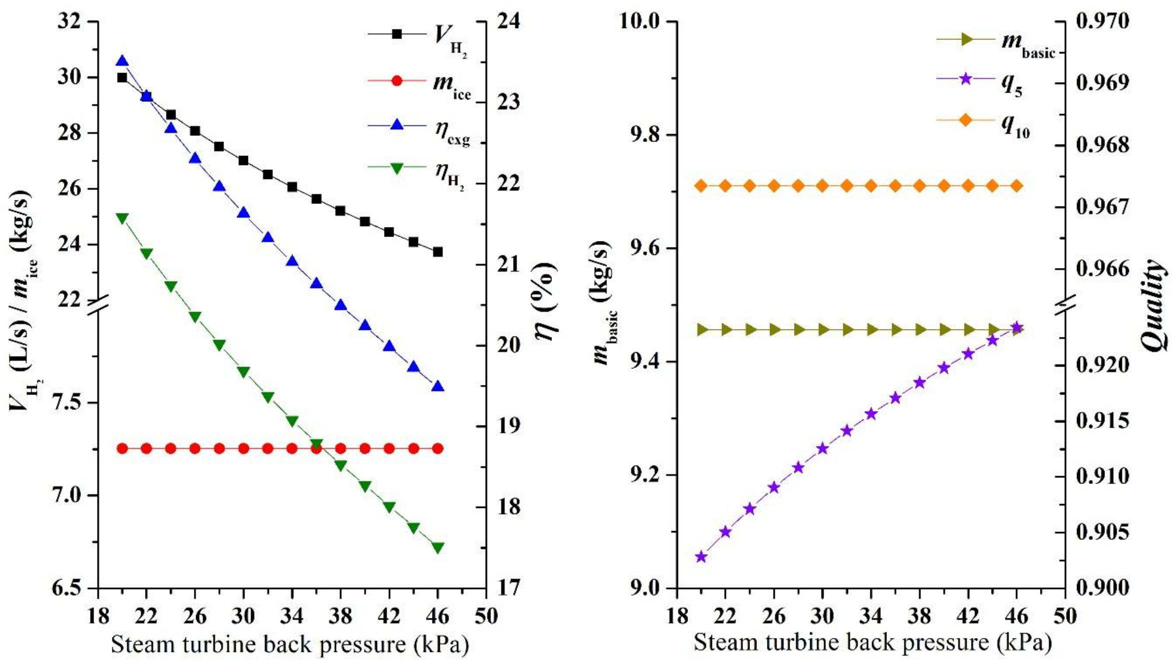

Fig. 4 The effect of steam turbine back pressure on the system performance

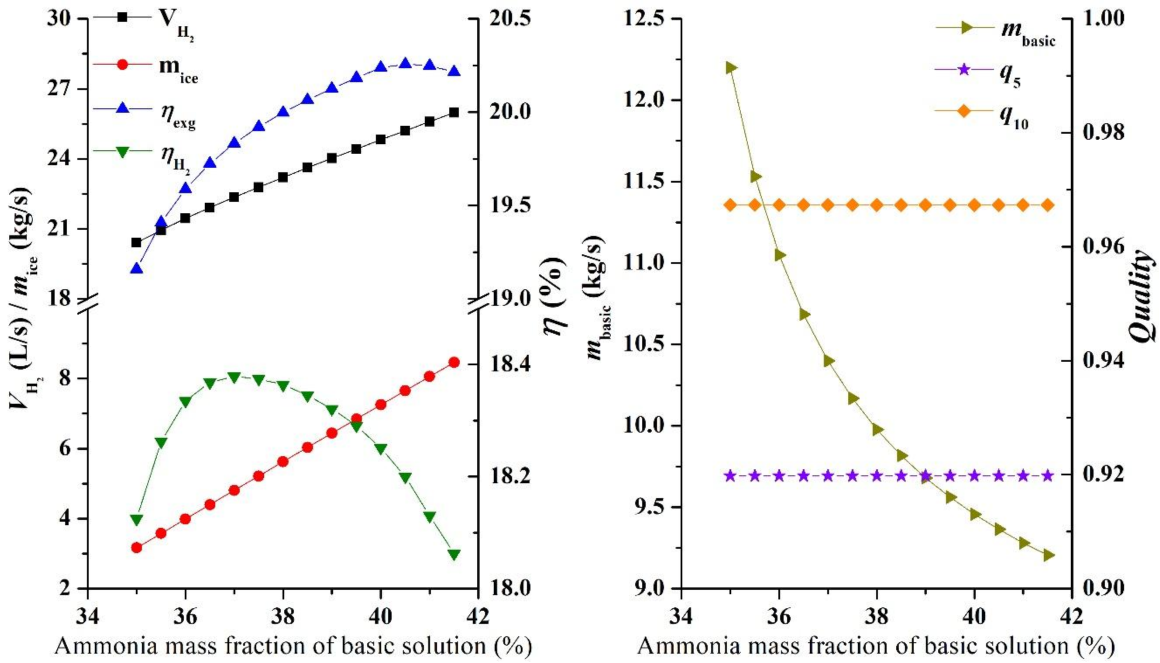

Fig. 5 The effect of ammonia mass fraction of basic solution on system performance

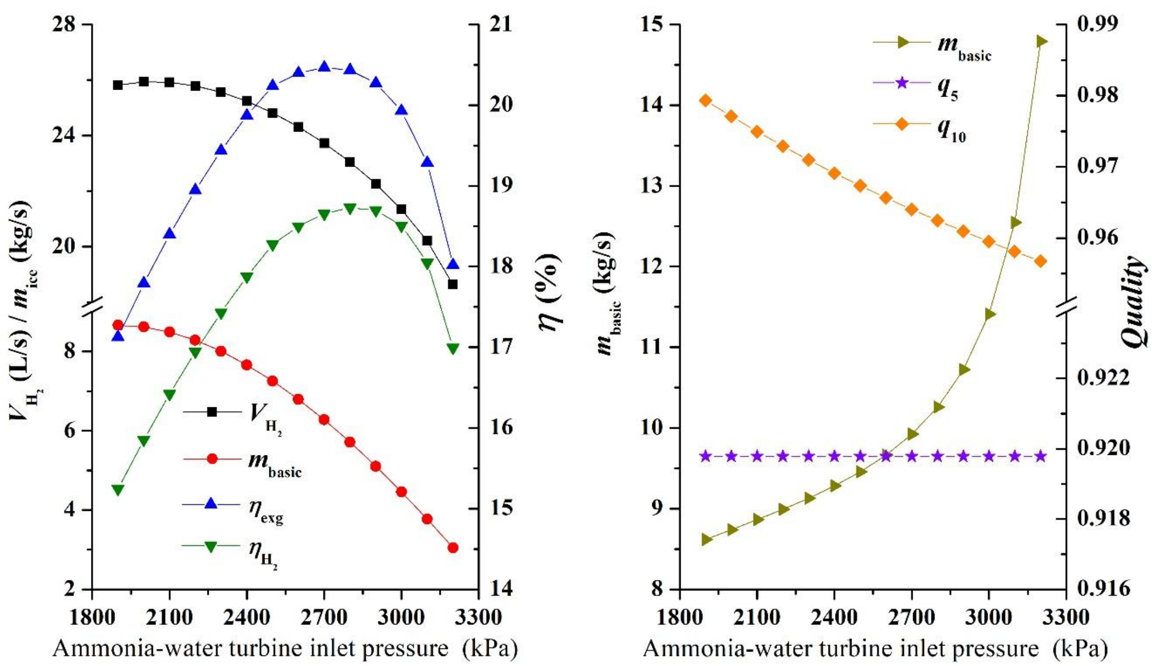

Fig. 6 The effect of ammonia-water turbine inlet pressure on system performance

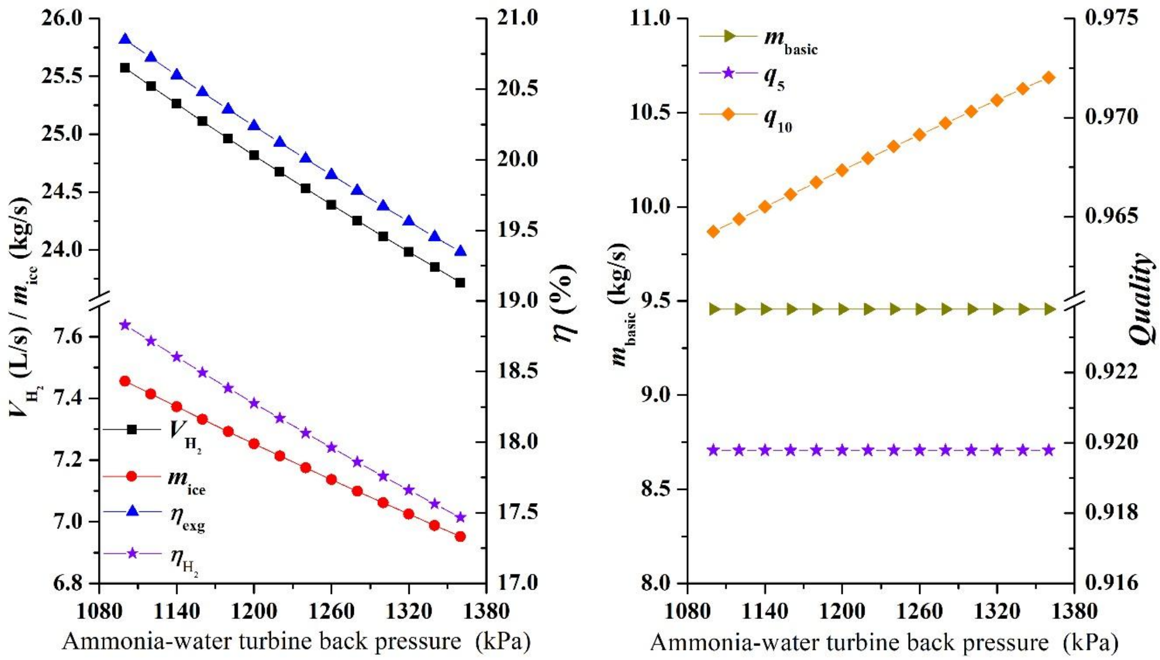

Fig. 7 The effect of ammonia-water turbine back pressure on system performance

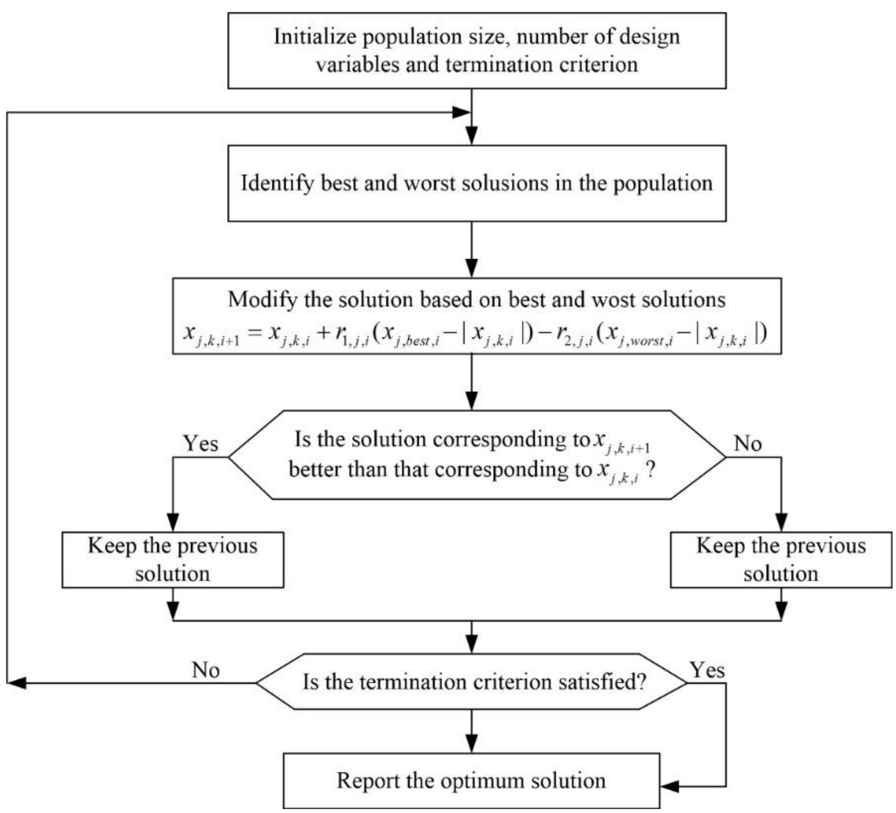

Fig. 8 The Flow chart of Jaya algorithm